von Karman Institute for Fluid Dynamics

Lecture Series 1991-08

Laser Velocimetry

June 10 - 14, 1991

Biasing Errors and Corrections

James F. Meyers
NASA - Langley Research Center
Hampton, Virginia, USA

Biasing Errors and Corrections

by

James F. Meyers
NASA - Langley Research Center
Hampton, Virginia 23602-5225
United States

Introduction

The inability to perfectly measure a physical process can be attributed to the lack of precision and accuracy of the measuring device and the affect of external influences on the overall accuracy of the measurement. Early instrumentation systems suffered from such poor precision that external influences were generally ignored. The advent of analog-to-digital converters helped the precision by reducing the sources of variability error inherent in analog systems to just the sensor. The converters however, added new problems by measuring a process only at discrete times requiring statistical estimates of that process, thus continuous tracking was no longer possible. With the increased precision, external influences now became important, especially the added influence of digital sampling. Mathematicians tell us there is no influence on the measurement statistics if the sampling is independent of the physical process. Thus one may obtain quality measurements by uniformly sampling a process because the digital clock typically used to drive analog-to-digital converters is independent of the process being sampled. The mathematicians further tell us that uniform sampling is not required, any clock with independent statistics will do, e.g., random walk, Gaussian, Poisson, etc.

During the advent of laser velocimetry, analog measurement techniques such as spectrum analyzers and frequency lock loops were used to measure the near continuous signals obtained from water flows. The digital frequency tracker was developed by using an analog-to-digital converter to sample the output from the frequency discriminator in a frequency lock loop. The increased control of the feedback loop by digital circuits operating on digital signals increased measurement precision and even reduced the requirement of near continuous input signals. The next logical step was to remove the frequency lock loop and directly digitize the individual signal burst obtained from a single particle passing through the laser velocimeter sample volume. Extensive studies of particle passage statistics indicated that their arrivals obeyed Poisson statistics regardless of the average rate.

Remembering that the mathematicians stated that Poisson statistics were an independent sampling process, researchers placed their laser velocimeters in air flows and reduced their seeding rates to tolerable levels with full confidence that this new method was the panacea of measurement techniques.

In 1973 McLaughlin and Tiederman, reference 1, of Oklahoma State University noticed that their mean velocity measurements of a turbulent boundary layer were consistently higher than theory predicted. Seeking to determine the cause of this discrepancy, they reasoned that a uniformly seeded volume would yield a greater number of particle passages per unit time through the sample volume as the velocity increased. Since the number of measurements of the higher velocities in the turbulent flow would be greater than the number from lower velocities, the statistical velocity mean would be weighted toward the higher velocities. Applying a weighting function of inverse velocity to the statistical calculations, their measurements agreed much closer to theory.

Now convinced that mathematicians should be barred from the real world, researchers began to apply the inverse velocity correction to all laser velocimetry data. It wasn't long before correction schemes were being developed faster than researchers could digest them. Techniques such as two-dimensional weighting, true velocity magnitude weighting, residence time weighting, and time averaging were being developed as the *true* correction scheme, reference 2. The only universally accepted truth was that all laser velocimeter data were in error and needed correcting.

Look Again, Something's Not Right

In 1982 Meyers and Wilkinson, reference 3, from NASA - Langley Research Center were tasked to prove that the laser velocimeter could be used to make turbulence intensity measurements of flow fields with acceptable accuracy. The test was conducted in the jet from a fully developed turbulent pipe flow using an orthogonal three component laser velocimeter, figure 1, with a hot wire placed 2 mm downstream of the sample volume to serve as the measurement standard, figure 2. The hot wire was calibrated in a particle laden, low turbulent jet placed just above the pipe flow, figure 3. The velocity of the calibration jet was adjusted, under computer control, to obtain the hot wire calibration with the laser velocimeter providing the mean velocity measurements at each velocity station. The seeding particles in both the calibration jet and the pipe flow jet were 0.5 micron polystyrene microspheres to insure particle tracking fidelity in the flow fields. The hot wire output was

digitized with each measurement converted to velocity through a spline fit calibration curve with the resulting ensemble statistically analyzed. The 15 m/sec flow was seeded sufficiently to yield an average data rate of 2,000 samples per second. True velocity vector measurements made by the three component laser velocimeter operating in full coincidence indicated an on-axis flow with small angular scatter until the entrained region was reached where the flow deviated slightly outward and the scatter increased to approximately ±10 degrees. The local turbulence intensity at this point was in excess of 30 percent. Thus the flow was one dimensional through the operating envelope of the hot wire. With the test conditions well defined, comparative testing began. Radial scans were made at several downstream locations from the exit of the jet. The local turbulence intensity values compared well within the core region of the jet, but deviated greatly in the entrained region, e.g., figure 4. The measured data were processed using standard statistical calculations:

$$U = \frac{\sum_i u_i}{N} \tag{1}$$

$$\sigma^2 = \frac{\sum_i (u_i - U)^2}{N} \tag{2}$$

Attempting to improve the comparative measurements, the one-dimensional weighting factor proposed by McLaughlin and Tiederman:

$$U = \frac{\sum_i A_i u_i}{\sum_i A_i} \tag{3}$$

$$\sigma^2 = \frac{\sum_i A_i (u_i - U)^2}{\sum_i A_i} \tag{4}$$

where

$$A_i = \frac{1}{u_i}$$

was applied to the laser velocimeter data, figure 5. Curiously, the comparisons within the core became worse while the comparisons in the entrained regions improved. This trend remained consistent at all scan positions downstream from the exit of the pipe flow.

Remembering that McLaughlin and Tiederman stated that a uniformly seeded flow will yield a greater number of particle passages per unit time through the measurement volume as velocity increases, biasing should have been present. Since the particles were added 66 pipe diameters upstream of the jet, full mixing should yield the necessary uniform spatial distribution within the fully developed turbulent flow, but the correction does not work. In the entrained region, the portion of the flow from the pipe contains many particles while the entrained flow has few particles. The seeding in this region is far from uniform, yet the correction appears to work.

The hypothesis that high velocity increases the data rate while lower velocities decrease the data rate implies a correlation between velocity and data rate. This correlation can be verified by calculating the standard correlation coefficient between any two processes:

$$C = \frac{<U - u_i><R - r_i>}{\sigma_u \, \sigma_r} \tag{5}$$

where U is the statistical mean velocity from the selected measurement ensemble and u_i is the i^{th} velocity during the shortest period of time considered to be independent from other times. This period of time is referred to as the Taylor time microscale and is the time that the flow takes to change one standard deviation:

$$T_\lambda = \frac{\sigma_v}{\left\{ <\left(\frac{dV}{dt}\right)^2>^{\frac{1}{2}} \right\}} \tag{6}$$

The brackets, < >, denote the expected value of the enclosed expression. There is an implicit assumption that stationary systems are being discussed so that no distinction is made between time averaging and ensemble averaging. The parameter σ_u is the flow root mean square variation. The Taylor microscale has also been described as the time scale over which there is no significant change in the energy of an eddy.

The variable R in equation (5) is defined as the statistical mean data rate during the acquisition of the selected measurement ensemble and r_i is the data rate during the i^{th} flow microscale. The simultaneous measurement of velocity with the hot wire provided the data necessary to determine the Taylor time microscale for each measurement ensemble in the radial scan. The velocity time history obtained with the laser velocimeter was divided into Taylor time microscales and the *instantaneous* velocities and rates calculated. Applying these values to equation (5) and normalizing by the standard deviations of velocity, σ_u,

and data rate, σ_r, the correlation coefficients were determined. The resulting coefficients, plotted in figure 6, indicate an independent sampling process in the center of the flow since the coefficients are near zero, and a dependence in the entrained region since the coefficients are greater than zero. Therefore the measurements within the core of the flow are indeed independent and the statistics should not be corrected whereas the measurements within the entrained flow are not independent and their statistics should be modified. This explains the behavior of the data comparisons.

While the results from these calculations indicate independence in the core region, the logical strength of the hypothesis is hard to ignore. Plotting the incremental correlation coefficients versus the difference between the *instantaneous* data rate and the average data rate during the corresponding Taylor time microscale results in the scatter pattern shown in figure 7. A correlation between velocity and data rate would result in a data grouping along a 45-degree line. A portion of the velocity and data rate time history for a series of microscales, also shown in figure 7, do not exhibit any pattern. Expanding the time history, figure 8, reveals a few microscales where velocity and data rate have the same trends, however the remaining microscales have opposing trends.

The investigation clearly illustrates that the simple correction schemes previously proposed are not applicable because they are based on the general assumption of uniform spatial seeding. The investigation shows that this assumption is not generally valid and even when it is, the sampling may still be independent and thus the data do not require correction. The correcting scheme must determine, based only on the measurement ensemble being processed, if correction is necessary, and if so, how much is required.

The first approach to be based only on the ensemble characteristics was the sample and hold processing technique developed by Dimotakis, reference 4, (backward step algorithm) and Edwards and Jensen, reference 5, (forward step algorithm). This technique develops a continuous velocity time history by holding a velocity measurement until the next velocity measurement is made in the manner of a sample and hold circuit. This technique can be implemented by either using interarrival time, Δt, as a weighting factor:

$$U = \frac{\sum_i u_i \, \Delta t_{i+1}}{\sum_i \Delta t_{i+1}} \tag{7}$$

$$\sigma^2 = \frac{\sum_i (u_i - U)^2 \, \Delta t_{i+1}}{\sum_i \Delta t_{i+1}} \tag{8}$$

or uniformly sampling of the time history at an arbitrary rate to develop the flow statistics. By uniformly sampling the time history, the particle arrival statistics are nullified and the resulting measurement statistics are correct. Using this technique to process the jet flow data improves the comparative measurements in both the core and entrained regions as shown in figure 9. Stevenson, Thompson, and Roesler, reference 6, approximate the sample and hold method by using a high particle density in the flow, coupled with a high-speed burst counter with a long reset time to obtain a saturated detector. Since this approach obtains a velocity measurement every time the burst counter is ready to acquire one, a uniform and thus unbiased sampling of the flow field is obtained. Unfortunately the data rates required to obtain a saturated detector are prohibitively high to be useful in normal wind tunnel applications. Even the sample and hold method should have a data rate greater than 10 measurements per Taylor time microscale to fully describe the velocity time history. Since the required data rate is dependent on the Taylor time microscale at each point in the flow, a method needs to be developed to estimate the microscale either during data acquisition or from the acquired data ensemble.

If it is assumed that the flow velocity remains near a given value during the Taylor time microscale, a method for estimating that time microscale can be developed as follows: Divide the velocity range of the selected data ensemble into ten velocity bins and overlay these bins on the velocity time history, figure 10. Based on the assumption, velocity measurements made within the microscale will remain in the same velocity bin, whereas measurements in successive microscales probably will be in other bins. Thus an estimate of the flow correlation time may be obtained by calculating the average residence time for the flow velocity to remain within a bin. Testing this technique using the data from the turbulent jet indicated that the average residence times were approximately 20-percent of the Taylor time microscales obtained from the hot wire. The required data rate can now be determined for the sample and hold technique based only on the measurement ensemble. The velocity : data rate correlation coefficient can be determined by using the average residence time to establish the *instantaneous* velocity and data rate, figure 11.

Calculation of Independent Statistics

Instead of adjusting the particle generator to obtain sufficient data rates to use the sample and hold method, it may be easier to use the Taylor time microscale and the knowledge that measurements in successive microscales are independent to develop a new technique to insure statistical independence of the data. A single velocity measurement within a correlation time should represent the flow velocity during that time and additional measurements give an indication of the particle arrival rate statistics for that velocity. Thus a second interrogation of the velocity time history can yield ensembles of independent velocity measurements, and particle arrival rates as a function of flow velocity. The method developed by Edwards and Meyers, reference 7, is based on two suppositions: (1) The velocity field is coherent during the Taylor time microscale following a measurement and thus additional measurements occurring during this time yield no further information. (2) The number of additional measurements yield an indication of the probability of occurrence of that measured velocity. The method is implemented by establishing two histograms, the normal velocity histogram of *measured* velocities and the occurrence histogram containing the number of *additional measurements* during the Taylor time microscale following each *measured* velocity. The first measurement in the velocity time history shown in figure 12 is located in bin 6 with two additional measurements within the following microscale. Thus the count in bin 6 of the velocity histogram is incremented by one and the count in bin 6 in the occurrence histogram is incremented by two. The first measurement following the microscale is also in bin 6 with three additional measurements following. Bin 6 in the velocity histogram is again incremented and bin 6 in the occurrence histogram is incremented by three. This procedure continues through the entire time history.

The acquired data for this example were obtained on the centerline of the jet with the resulting raw data histogram shown in figure 13. Following data interrogation, the resulting histogram of *measured* velocities obtained from the measurement ensemble is shown in figure 14. The velocity histogram is then used to normalize the occurrence histogram yielding the average number of measurements in the microscale following the *measured* velocity as a function of velocity, figure 15. The figure shows the normalized occurrence histogram to be approximately flat indicating no velocity is favored in the sampling process over the others. Therefore it is expected that the correlation coefficient between velocity and data rate will be low, as was found to be the case, figure 6. If the hypothesis by McLaughlin and Tiederman was correct, the normalized occurrence histogram would approximate a ramp function with the highest value located at the highest velocity.

The final step in the data processing scenario is to divide the normalized occurrence histogram into the *measured* velocity histogram to yield a normalized velocity histogram with all sampling biases removed, figure 16, and to perform the desired statistics on the resulting distribution. A second example ensemble obtained near the edge of the jet is presented to illustrate the procedure with measurements of a highly turbulent flow field. The raw data histogram, normalized occurrence histogram, and normalized velocity histogram are shown in figures 17, 18, and 19 respectively. The normalized occurrence histogram is basically flat with a small rise toward higher velocities indicating a small velocity bias. This is verified by a velocity : data rate correlation coefficient of 0.029 obtained for this ensemble. The results of processing the pipe flow measurements using this technique are shown in figure 20. The ensuing comparison with the hot wire data is superior to the other techniques employed.

Vortex Flow Above a 75° Delta Wing

Now that the presence of velocity bias can be determined using the velocity : data rate correlation and a procedure has been developed to obtain an independent data set from a velocity measurement ensemble, it is appropriate to study a more complicated flow field than the turbulent pipe flow jet. The flow selected was the leading edge vortex flow field above a 75° delta wing, reference 8. The selection is appropriate since this fundamental flow is utilized in many high performance aircraft designs to increase the flight performance envelope. A leading edge vortex pair contains a great deal of energy which, if carefully controlled, can provide significant lift on an aircraft. However, if a vortex is disturbed it will burst, dissipating its energy in a random manner resulting in a sudden loss of lift. This problem is of special concern for aircraft stability when only one vortex of a coupled pair bursts, resulting in sudden substantial rolling moments being applied to the aircraft.

The model is a 75° swept delta wing with a 0.305 meter span and sharp leading edges (10° bevel on the lower surface with the upper surface flat). A 20.5° angle of attack yields a stable vortex flow above the model. An increase to 40.0° causes the vortex flow to burst over the model. The tunnel speed is adjusted to obtain a chord Reynolds number of 1.0 million for both conditions. The investigations were conducted in a plane orthogonal to the surface of the model at an $x/L = 0.7$.

The flow above the delta wing at an angle of attack of 20.5° consists of two stable leading edge vortices. A laser light sheet visualization of these vortices is shown in figure 21. The three component mean velocity

measurements obtained with the laser velocimeter at 20.5° angle of attack are shown in figure 22. It is noted that the streamwise component increases to twice free stream velocity within the core of the vortex. The vortex flow is very stable which should yield long Taylor time microscales in the core region. The contour map of the estimated microscales is shown in figure 23 and indeed the core regions are very distinctive with their long microscales. Contours of the velocity : data rate correlation, shown in figure 24, have no discernible pattern nor are the coefficients large enough to indicate significant velocity bias.

If the angle of attack is increased to 40.0°, the vortices burst. The velocity measurements shown in figure 25 indicate that the streamwise component reverses while the circulation velocity remains intact. This unstable flow would be expected to have short Taylor time microscales. The estimates, shown in figure 26, support this expectation with no evidence of any flow structure. Again the contours of the velocity : data rate correlation, shown in figure 27, have small coefficients indicating no discernible velocity bias, although a minor pattern does appear to be present.

Shear Flow Field Downstream of a Backward Facing Step

When making a comparative investigation between various techniques, the relative merit of each is best determined by applying them to the same flow field. A classic flow used by several researchers to determine the capability of a velocity bias correction technique is the flow downstream of a backward facing step. Adams and Eaton, reference 9, tested the time average approach (similar to the sample-and-hold method) while Stevenson, Thompson, and Roesler, reference 6, tested the use of a saturated detector. Since these investigations indicated the presence of velocity bias, a backward facing step was constructed, reference 10. The flow field was interrogated with a three component laser velocimeter. The data was processed using standard statistics and the histogram method developed by Edwards and Meyers. One and three component versions of the McLaughlin and Tiederman correction scheme were used as a reference.

The backward facing step facility, illustrated in figure 28 and shown in figure 29, is a suction facility with air being pulled through a single screen and honeycomb followed by four additional screens down a flat section 16 step heights long to a step expansion of 2:1 and an aspect ratio of 12:1. The inlet flow had a free stream velocity of 4.5 m/s and a turbulence intensity, measured by a hot wire of 1.2 percent. The Reynolds number was 650 based on the momentum thickness of the boundary layer at the step. The Reynolds number based on step height

was 22,200 and the displacement thickness of the boundary layer at the step was 0.35 step height. Polystyrene particles, 0.8 microns in diameter, were injected via atomization of a 50:50 mixture of ethanol and water in the air being pulled into the facility. Oscilloscope observations of the signal bursts indicated only monodisperse particles were passing through the measurement volume.

The laser velocimeter, shown in figure 29, was a four component system using a single Argon ion laser. The 488.0 nm line was selected and input to fiber optics and transmitted to a single component system located just downstream of the final screen. This fixed system measured the velocity along the centerline of the facility and provided the reference free stream velocity and data rate measurements and baseline particle arrival statistics. The remaining three components using the 514.5 nm, 496.5 nm, and 476.5 nm lines comprised the measurement system. The measurement system, illustrated in figure 30, used orthogonal transmission optics rotated 45 degrees to obtain direct three component measurements through a single window. A single optical receiver, using chromatic filtering for component separation, located perpendicular to the facility collects the scattered light. The focal length was 0.5 m with f-8.5 collecting optics yielding a spherical sample volume 100 microns in diameter. High-speed burst counters processed the signals from the three measurement components. A LVABI data acquisition system, reference 11, acquires the digital measurements from the three counters and passes the data ensembles to a minicomputer for final data processing and storage. The free stream component is processed by a burst counter in free run mode with direct input to the microcomputer used to monitor the facility parameters. The free stream results are passed to the minicomputer upon demand when the measurement ensembles are obtained.

A detailed vertical traverse was conducted three step heights downstream of the step. The velocity scan was made with the three laser velocimeter components in full coincidence and the velocity vector of each particle determined. This provided the velocity vector magnitudes required for the three-dimensional correction. As shown in figure 31, the determination of the mean velocity profile using the basic statistics and the histogram method track closely. The one-dimensional correction caused the velocities to deviate considerably behind the step whereas the three-dimensional correction moved the velocities closer to the basic statistics. The standard deviations of velocity normalized by the free stream velocity accentuates the differences between the basic statistics and the McLaughlin and Tiederman corrections, figure 32. Since the histogram method continues to track the basic statistics, the correlation coefficient between velocity and data rate is expected to be small. The velocity : data rate correlation coefficient, plotted in

figure 33, is indeed small with the maximum magnitude of 0.16 whereas the coefficient for the pipe flow data, figure 6, was up to a value of 0.3. However, the trend of the data is interesting. The correlation increases to a peak in the free shear layer where the heavily seeded high speed flow is mixing with the lightly seeded recirculating flow. The correlation then decreases to a negative peak in the shear region between the recirculation and the boundary layer indicating the slower boundary layer contains the greater number of particles. The flow Taylor time microscale, plotted in figure 34, is constant above the step then makes a smooth transition to a value three times longer behind the step. A marked increase in correlation time is then seen within the boundary layer behind the step.

An overall view of the flow field was made by measuring the velocities over a 0.5-inch grid from 1-inch upstream to 24-inches downstream of the step. The laser velocimeter was run in noncoincidence mode to increase the data rate especially in the separated region behind the step. The basic statistics, the histogram method, and the 1-dimensional bias correction results are shown for the mean velocity in figures 35-37 respectively and figures 38-40 respectively for the standard deviations normalized by the local mean velocity. Again the basic statistics and the histogram method have comparable results whereas the 1-dimensional bias corrected data deviates considerably from them, especially behind the step.

The velocity : data rate correlation coefficient map is shown in figure 41. If the correlation coefficients nine inches downstream of the step are compared to the corresponding data in figure 33, one notices major differences between the two data sets. Apparently the recirculation zone has gained significant numbers of particles, reversing the previous trends. A repeat of the vertical scan which yielded the data for figure 33, was performed with the same instrumentation settings used for the flow field mapping. A comparison of these two scans in figure 42 show similar results above the step, however the trends behind the step have opposite phases. This indicates that the heaviest particle concentration was within the recirculation zone. In reality this apparent change in the particle distribution is attributed to instrumentation settings. During the first scan, the reset time was adjusted from the normal 75 μsec to 300 μsec when the measurement volume was in the recirculation region. During the flow field mapping, the reset time was held at 75 μsec for all measurement locations. When the mean velocity slowed in the shear regions, the short reset time allowed the high-speed burst counters to obtain two or more measurements from the same Bragg-shifted signal burst. These extra measurements had no effect on the resulting velocity statistics because the correlation was so low, however they did cause the 180 degree phase shift in the correlation data. These results clearly

show the sensitivity of the velocity : data rate correlation to changes in the experiment, including the instrumentation.

Summary

The dependence of laser velocimeter measurement rate on flow velocity was first described by McLaughlin and Tiederman in 1973. They proposed that the dependency was a direct result of the fluid mechanics in the flow. In 1983, Edwards and Jensen investigated the possibility that the dependency was statistical and not directly coupled to flow velocity. This possibility was strengthened in 1984 by Edwards and Meyers when reviewing the data obtained earlier by Meyers and Wilkinson which simultaneously acquired three component laser velocimeter and hot wire data. Using the standard equation to determine the correlation between two parameters, this data proved that the ensemble was an independent sampling of the flow velocity field in the jet exiting from a fully developed turbulent pipe, a flow fully satisfying the assumption made by McLaughlin and Tiederman. Further investigations outlined in this lecture have shown that any dependence is purely statistical, and is nonstationary both spatially and temporally. The only patterns found were in mixing regions where two flows of different velocities containing different particle densities interact. Examples of these mixing regions include the entrained flow at the edge of a jet, and the strong shear region above a separation zone. The main conclusions to be drawn are that the times between successive particle arrivals should be routinely measured and the calculation of the velocity : data rate correlation coefficient should be performed to determine if a dependency exists. If none is present, accept the data ensemble as an independent sample of the flow. If a dependency is found, the data should be modified to obtain an independent sample. Universal correcting procedures should never be applied because their underlying assumptions are not valid.

References

1. McLaughlin, D. K.; and Tiederman, W. G., Jr.: *Biasing Correction for Individual Realization of Laser Anemometer Measurements in Turbulent Flow*. The Physics of Fluids, 16, 12, pp. 2082-2088, 1973.

2. Edwards, R. V., editor: *Report of the Special Panel on Statistical Particle Bias Problems in Laser Anemometry*. J. Fluid. Engr., vol. 109, pp. 89-93, June 1987.

3. Meyers, J. F.; and Wilkinson, S. P.: *A Comparison of Turbulence Intensity Measurements Using A Laser Velocimeter and A Hot Wire In A Low Speed Jet Flow*. Proceedings of the International Symposium on Applications of Laser-Doppler Anemometry to Fluid Mechanics, Lisbon, Portugal, paper 17.4, June 5-7, 1982.

4. Dimotakis, P. E.: *Single Scattering Particle Laser Doppler Measurements of Turbulence*. Applications of Non-Intrusive Instrumentation to Fluid Flow Measurement, AGARD CP-193, 1976.

5. Edwards, R. V.; and Jensen, A. S.: *Particle Sampling Statistics in Laser Anemometers: Sample-and-Hold Systems and Saturable Systems*. J. Fluid Mech., vol. 133, pp. 397-411, 1983.

6. Stevenson, W. H.; Thompson, H. D.; and Roesler, T. C.: *Direct Measurement of Laser Velocimeter Bias Errors in a Turbulent Flow*. AIAA Journal, 20, pp. 1720-1723, 1982.

7. Edwards, R. V.; and Meyers, J. F.: *An Overview of Particle Sampling Bias*. Proceedings from the Second International Symposium on Applications of Laser Anemometry to Fluid Mechanics, Lisbon, Portugal, paper 2.1, 1984.

8. Meyers, J. F.; and Hepner, T. E.: *Measurement of Leading Edge Vortices from a Delta Wing Using a Three Component Laser Velocimeter*. AIAA 15th Aerodynamic Testing Conference, San Diego, CA, paper AIAA-88-2024, May 18-20, 1988.

9. Adams, E. W.; and Eaton, J. K.: *An LDA Study of the Backward-Facing Step Flow, Including the Effects of Velocity Bias*. Proceedings of the International Symposium on Laser Anemometry, Winter Annual Meeting of the American Society of Mechanical Engineers, Miami Beach, FL, FED-Vol. 33, November 17-22, 1985, pp. 255-264.

10. Meyers, J. F.; Kjelgaard, S. O.; and Hepner, T. E.: *Investigation of Particle Sampling Bias in the Shear Flow Field Downstream of a Backward Facing Step*. Proceedings of the Fifth International Symposium on Applications of Laser Techniques to Fluid Mechanics, Lisbon, Portugal, paper 29.1, July 9-12, 1990.

11. Cavone, A. A.; Sterlina, P. S.; Clemmons, J. I., Jr.; and Meyers, J. F.: *A High Speed Buffer for LV Data Acquisition*. Proceedings of the 12th International Congress on Instrumentation in Aerospace

Simulation Facilities, College of William and Mary, Williamsburg, VA, pp. 113-120, 1987.

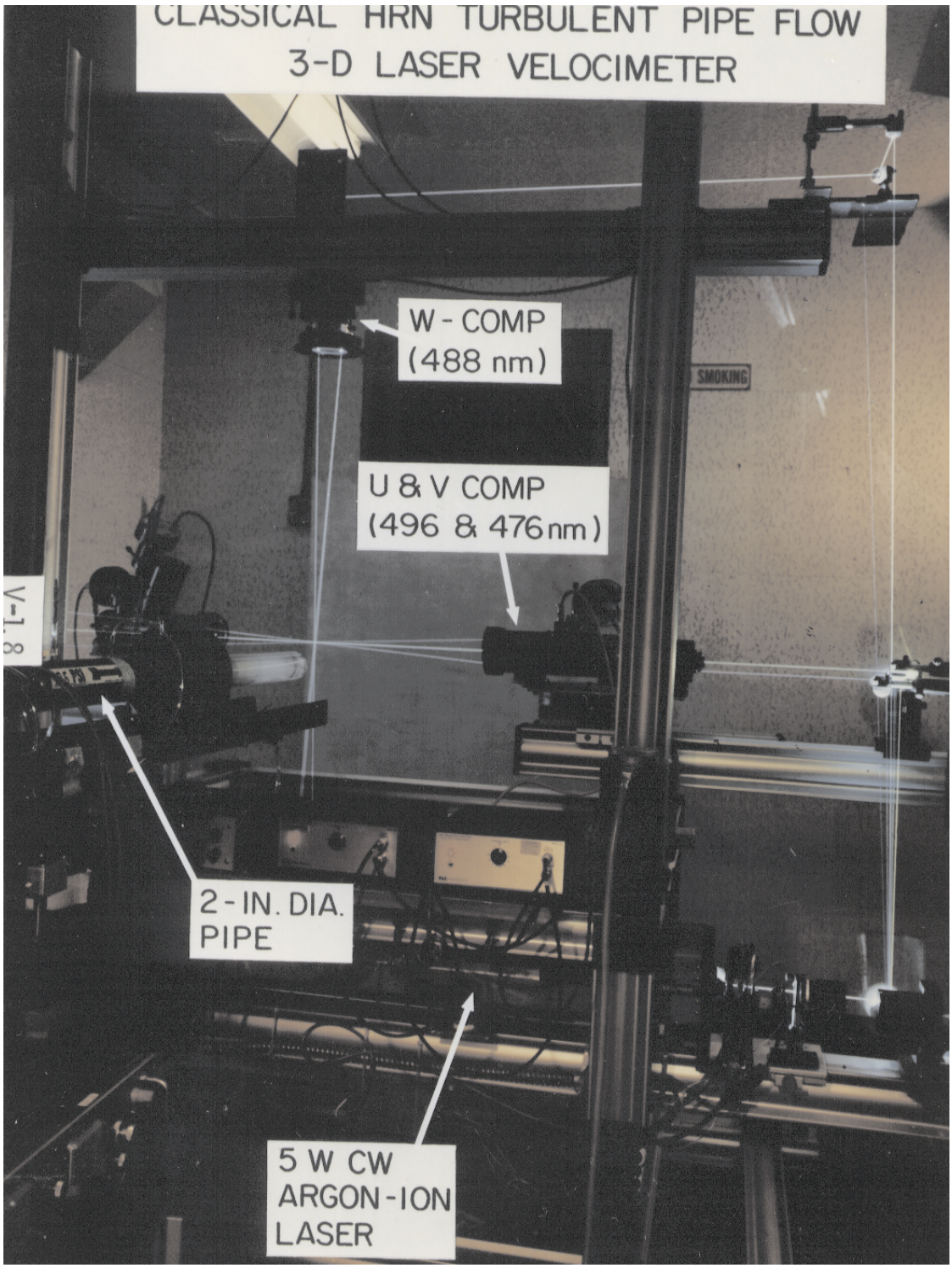

Figure 1.- Orthogonal three component laser velocimeter and the 5.0 cm diameter pipe.

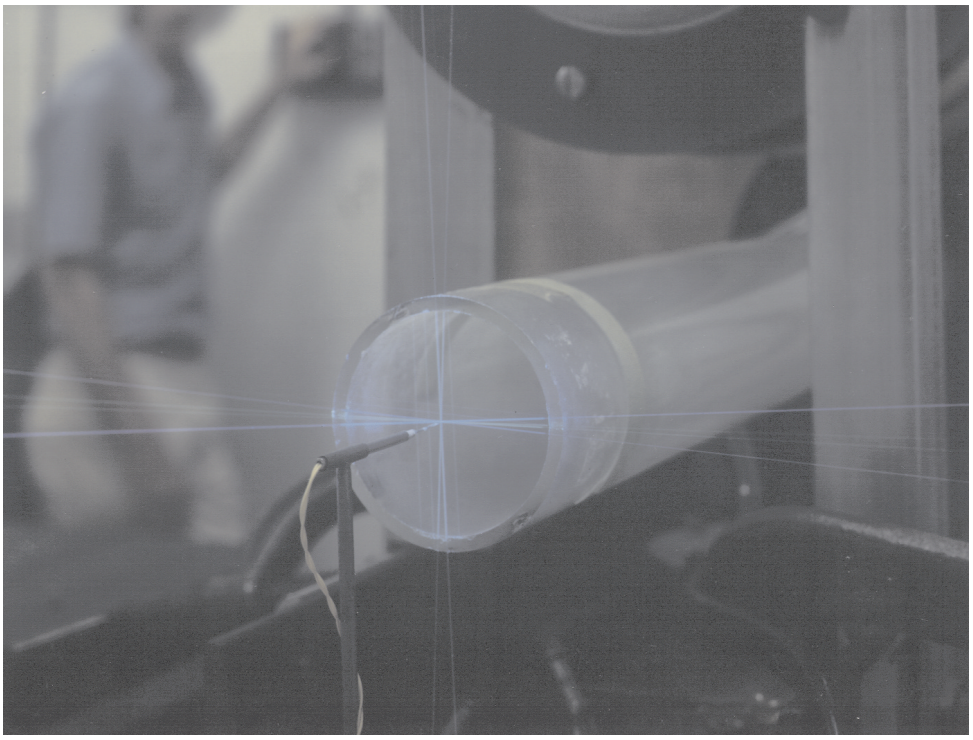

Figure 2.- Relative positions of the three component laser velocimeter measurement volume and the hot wire in the jet exiting from a fully developed turbulent pipe flow.

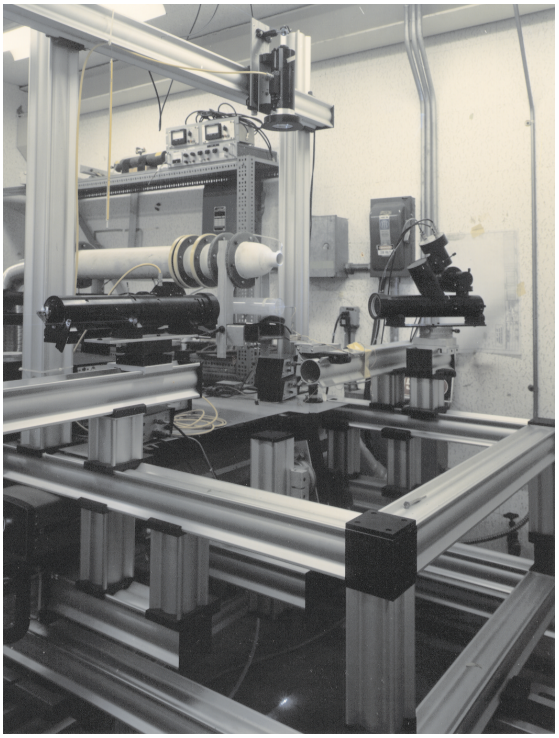

Figure 3.- View of the 5.0 cm diameter pipe and the low turbulence hot wire calibration jet facility.

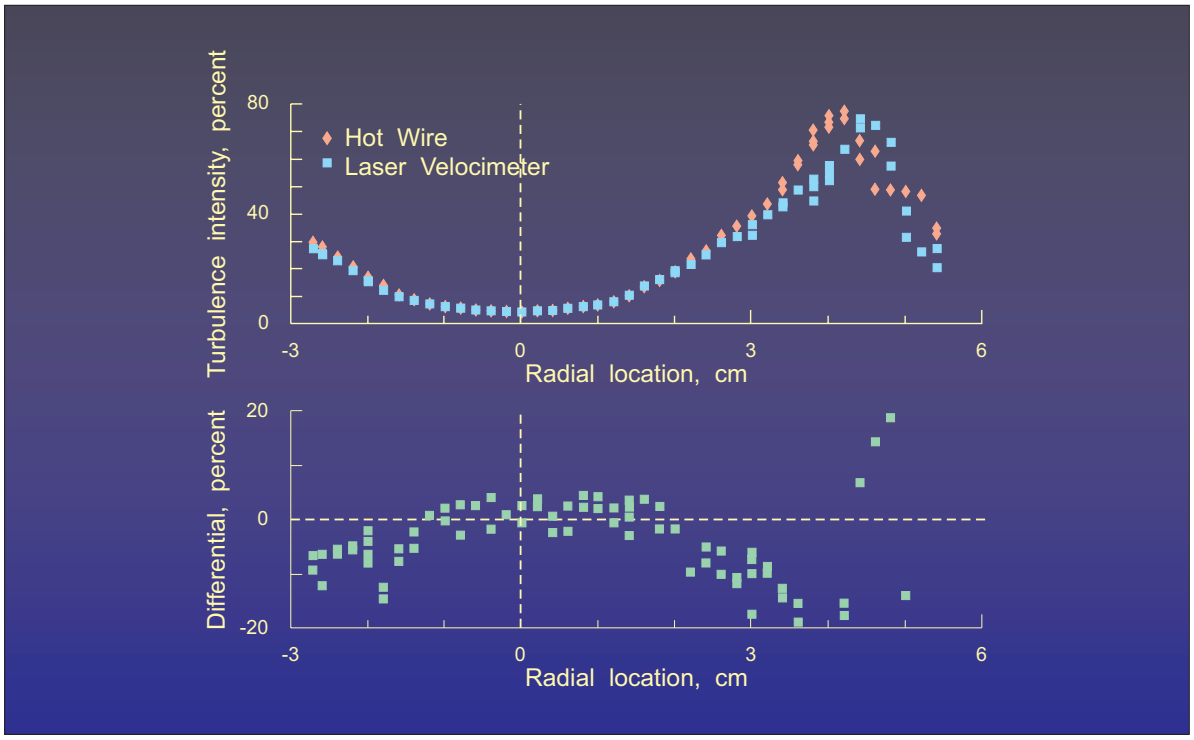

Figure 4.- Comparison of laser velocimeter and hot wire turbulence intensity measurements along a radial scan 12 cm downstream from the pipe exit.

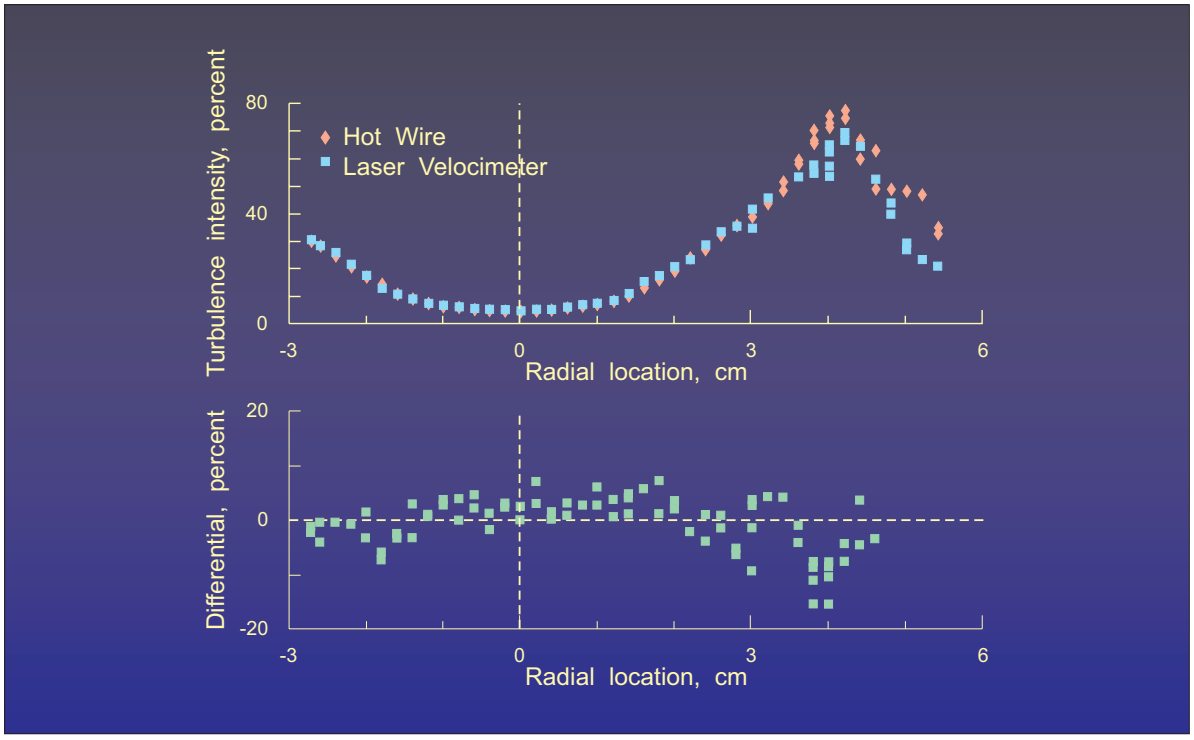

Figure 5.- Comparison of corrected (McLaughlin and Tiedermann) laser velocimeter and hot wire turbulence intensity measurements along a radial scan 12 cm downstream from the pipe exit.

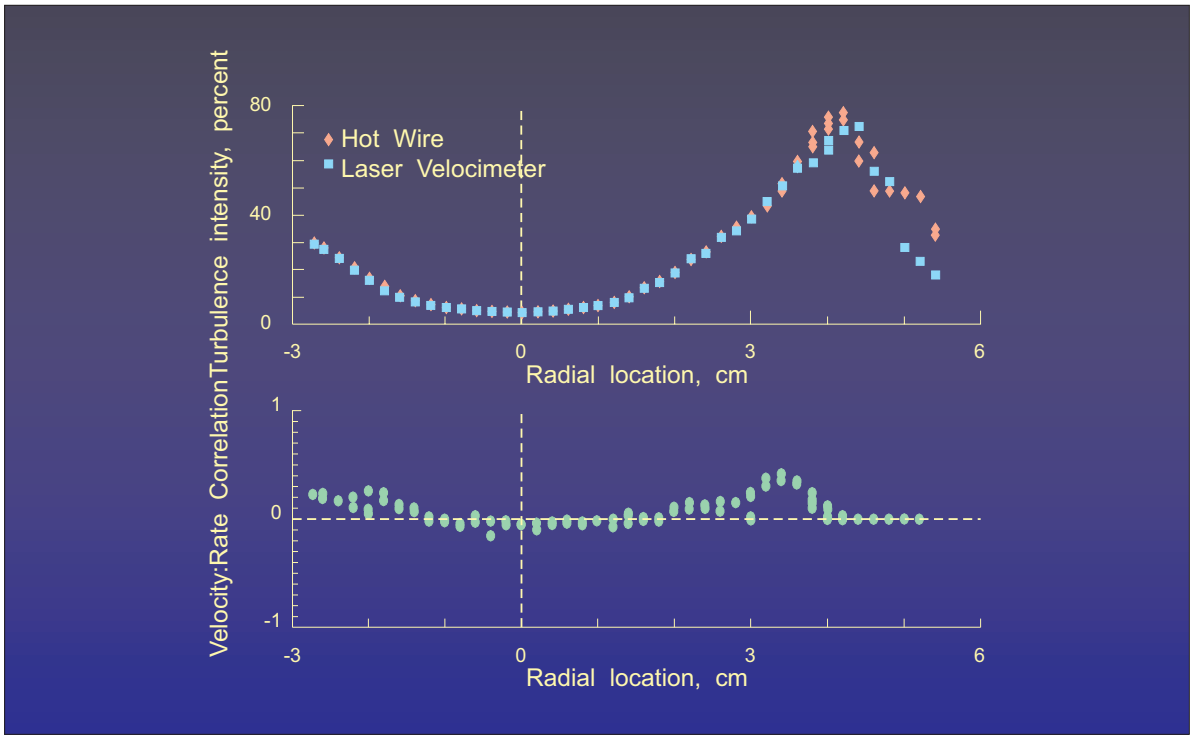

Figure 6.- Velocity : data rate correlation coefficients along a radial scan 12 cm downstream from the pipe exit.

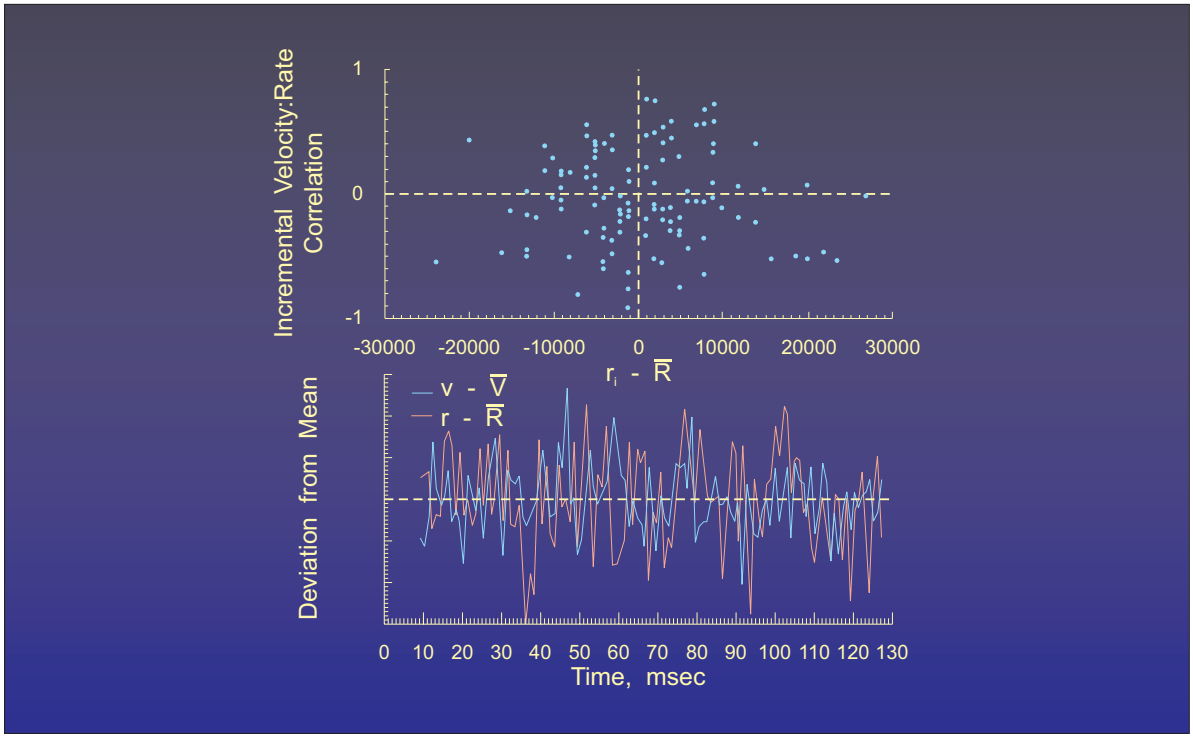

Figure 7.- Examination of incremental velocities and data rates from the laser velocimeter measurement ensemble obtained along the centerline of the pipe, flow 12 cm downstream from the pipe exit.

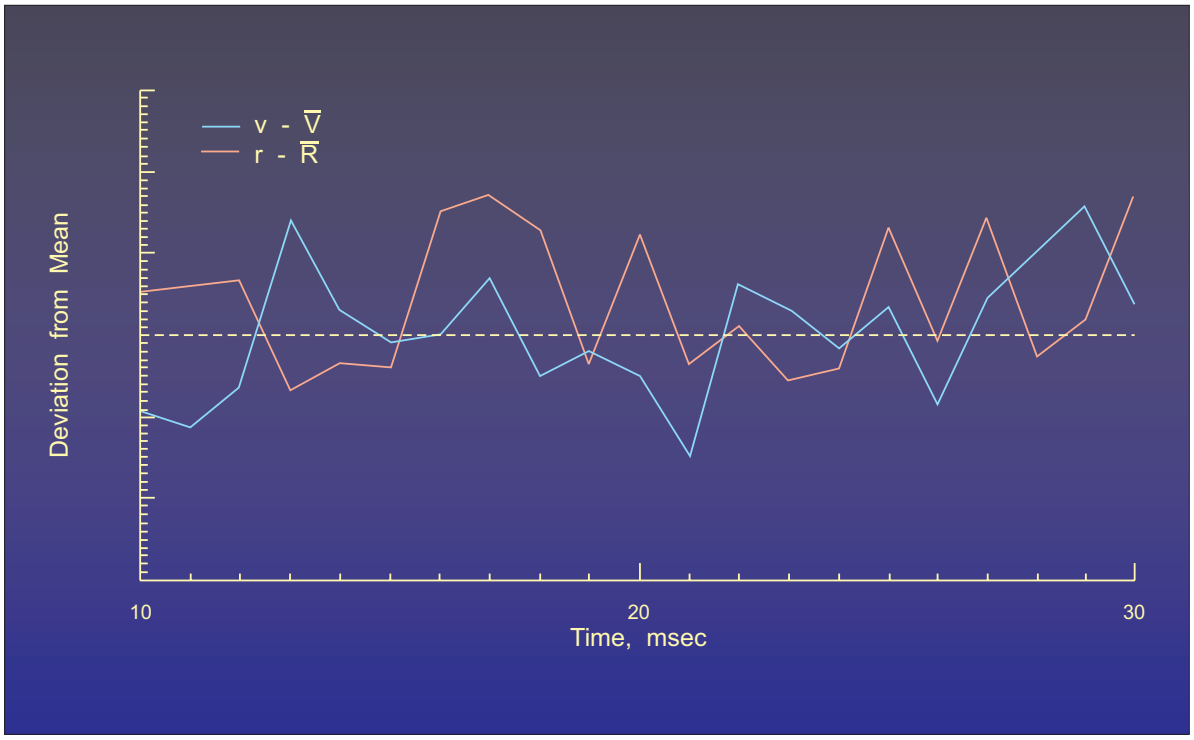

Figure 8.- Detailed examination of incremental velocities and data rates from the laser velocimeter measurement ensemble as a function of time.

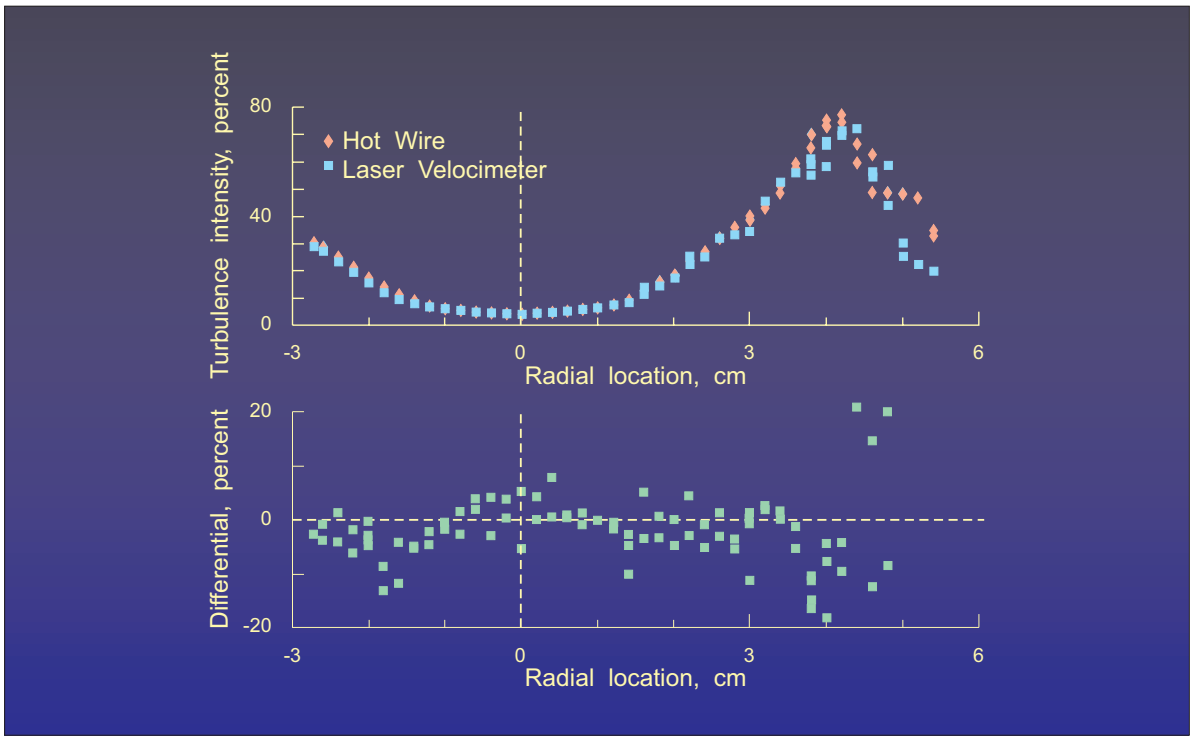

Figure 9.- Comparison of corrected (sample and hold processing) laser velocimeter and hot wire turbulence intensity measurements along a radial scan 12 cm downstream from the pipe exit.

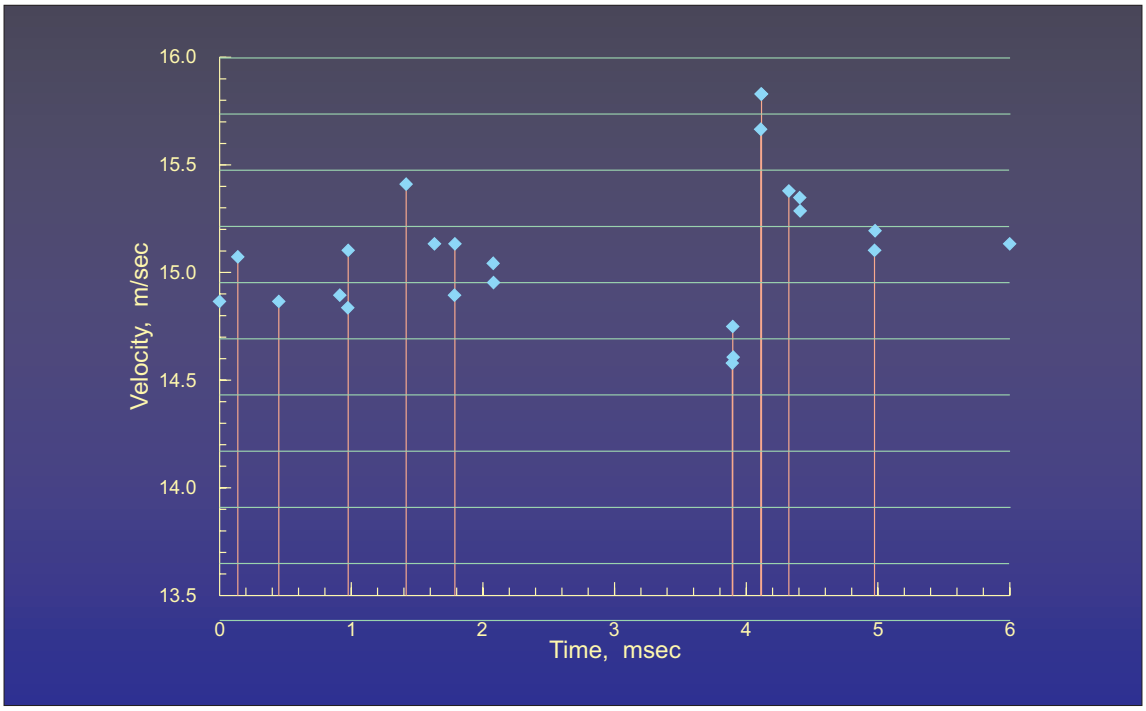

Figure 10.- Measured velocity time history of the measurement ensemble obtained along the centerline of the pipe flow, 12 cm downstream from the pipe exit used to estimate the Taylor time microscale of the ensemble.

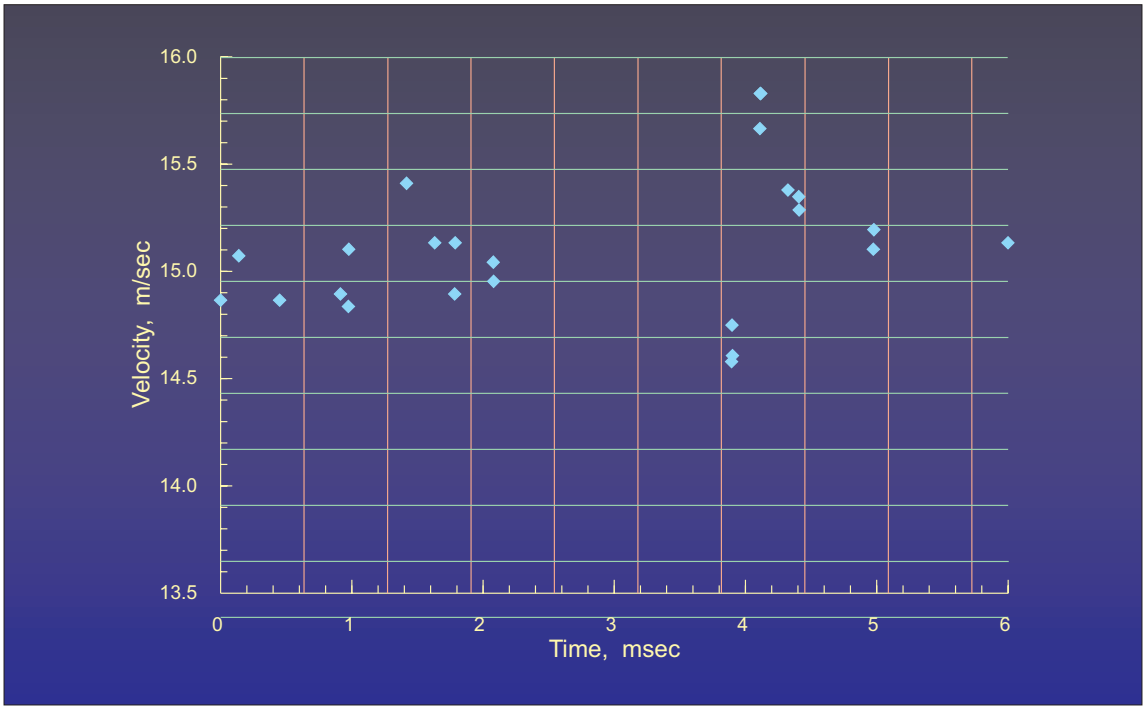

Figure 11.- Division of the velocity time history of the measurement ensemble obtained along the centerline of the pipe flow, 12 cm downstream from the pipe exit into Taylor time microscales to obtain the statistics required to calculate the velocity : data rate correlation coefficient.

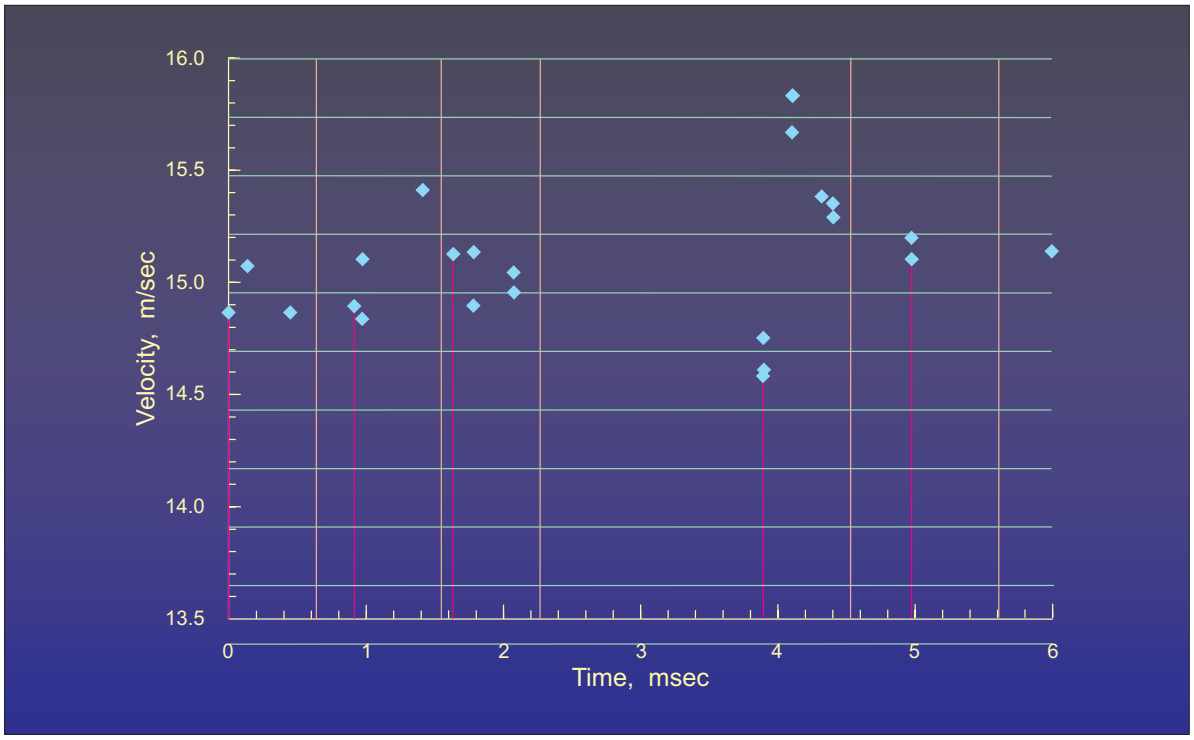

Figure 12.- Determination of independent measurement samples from the velocity time history of the measurement ensemble obtained along the centerline of the pipe flow, 12 cm downstream from the pipe exit.

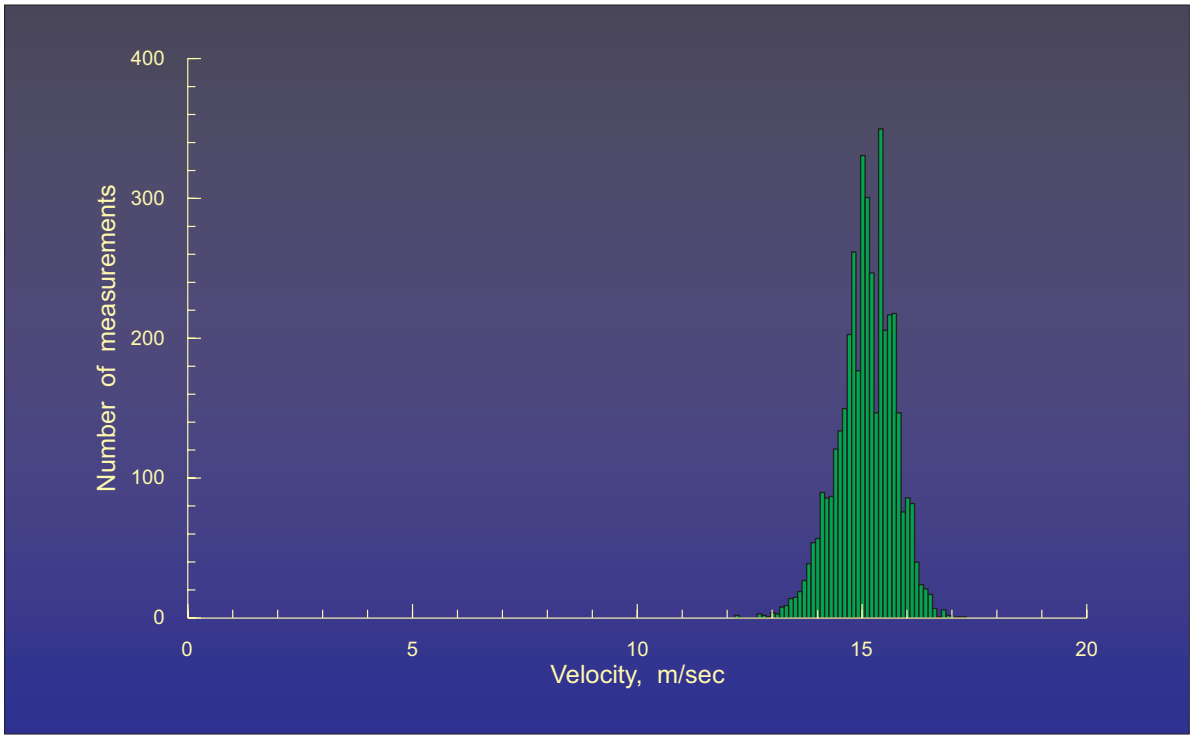

Figure 13.- Histogram of velocity measurements obtained along the centerline of the pipe flow, 12 cm downstream from the pipe exit.

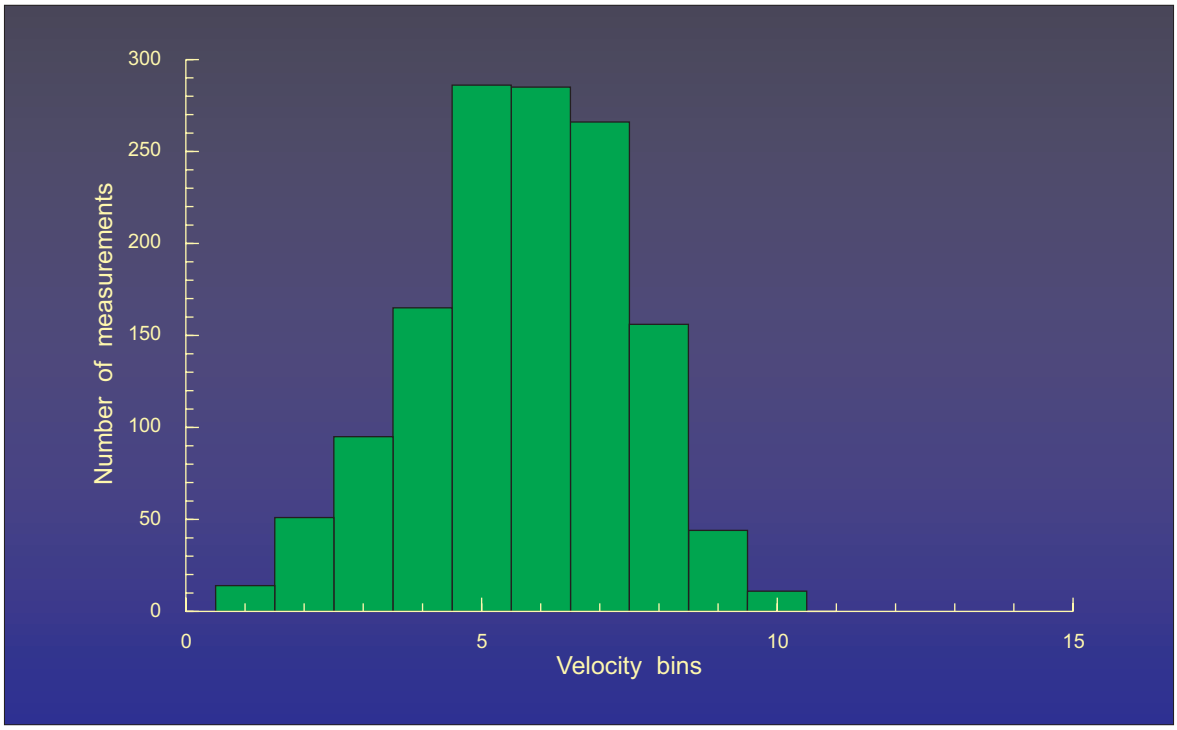

Figure 14.- Histogram of *measured* (first velocity measurement within a Taylor time microscale) velocities obtained along the centerline of the pipe flow, 12 cm downstream from the pipe exit.

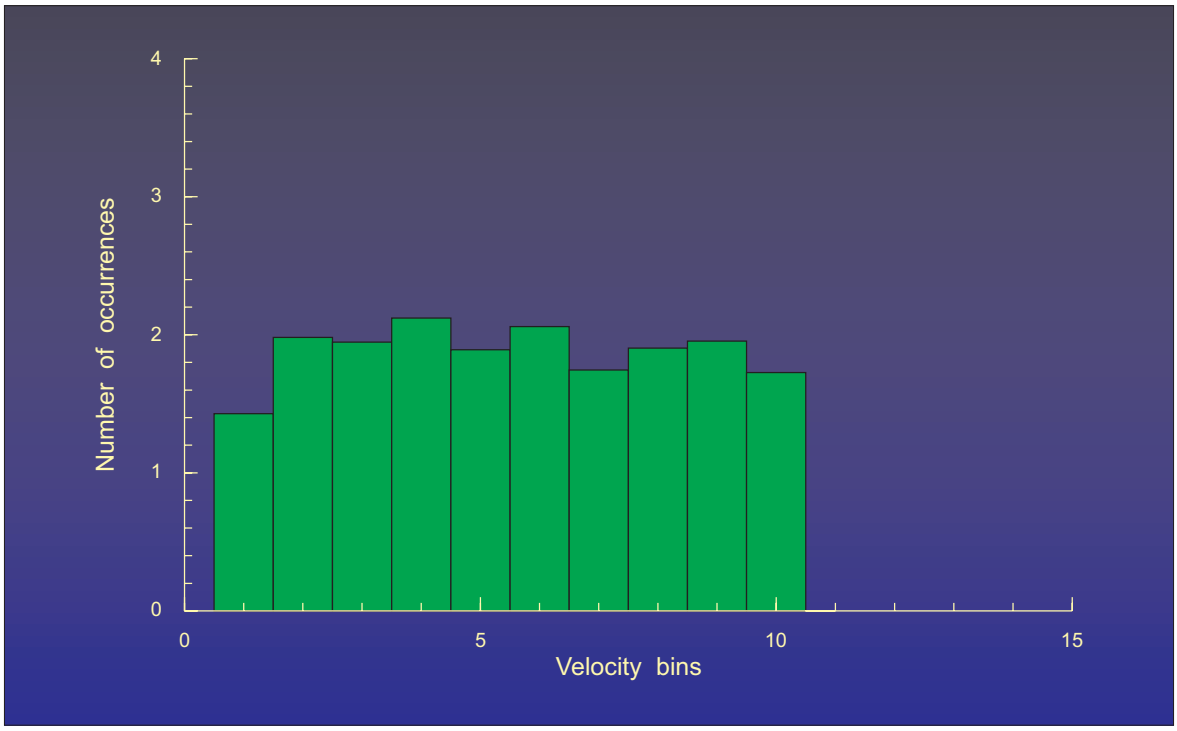

Figure 15.- Occurrence histogram of *additional measurements* following the first velocity measurement within a Taylor time microscale obtained along the centerline of the pipe flow, 12 cm downstream from the pipe exit.

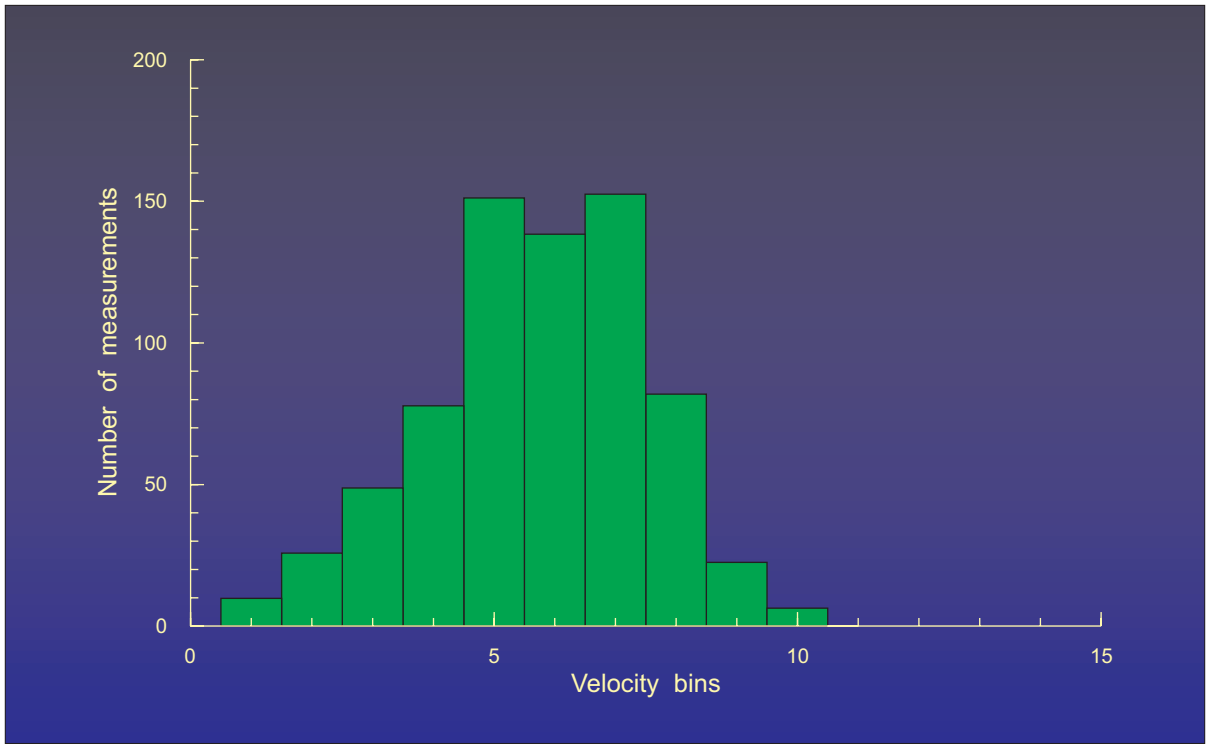

Figure 16.- Histogram of independent velocities obtained along the centerline of the pipe flow, 12 cm downstream from the pipe exit.

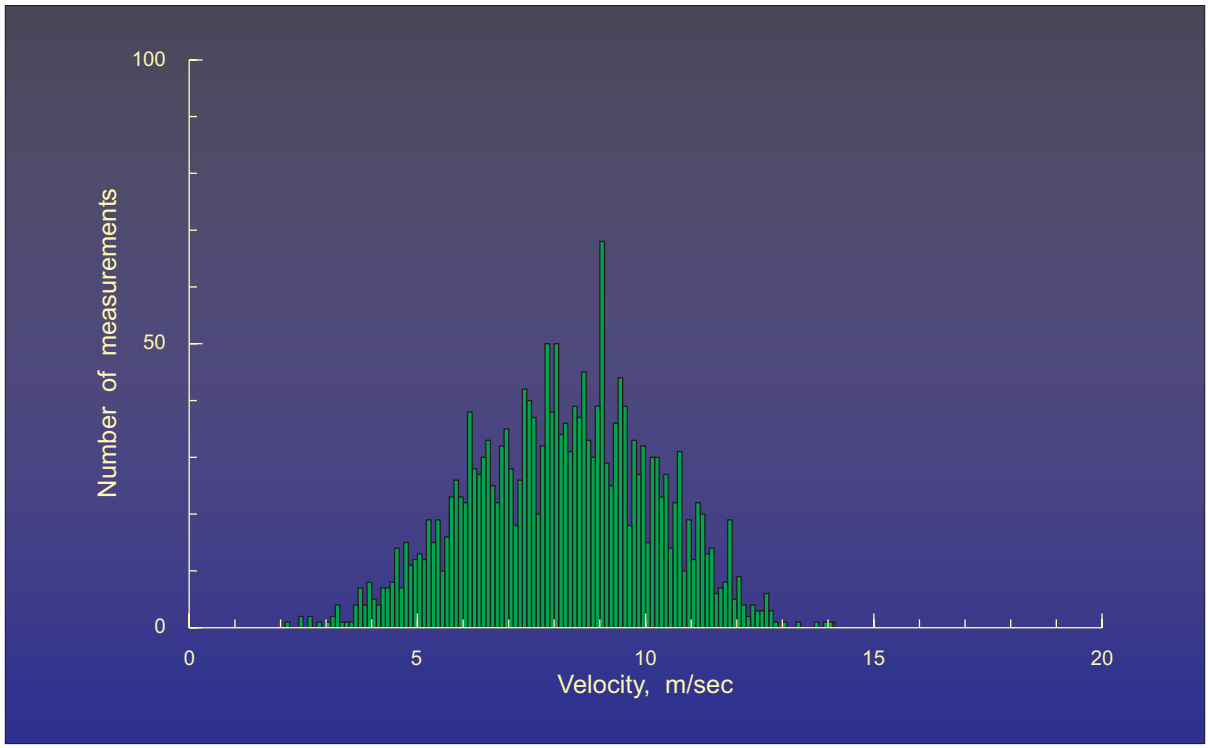

Figure 17.- Histogram of velocity measurements obtained at the edge of the pipe flow jet, 12 cm downstream from the pipe exit.

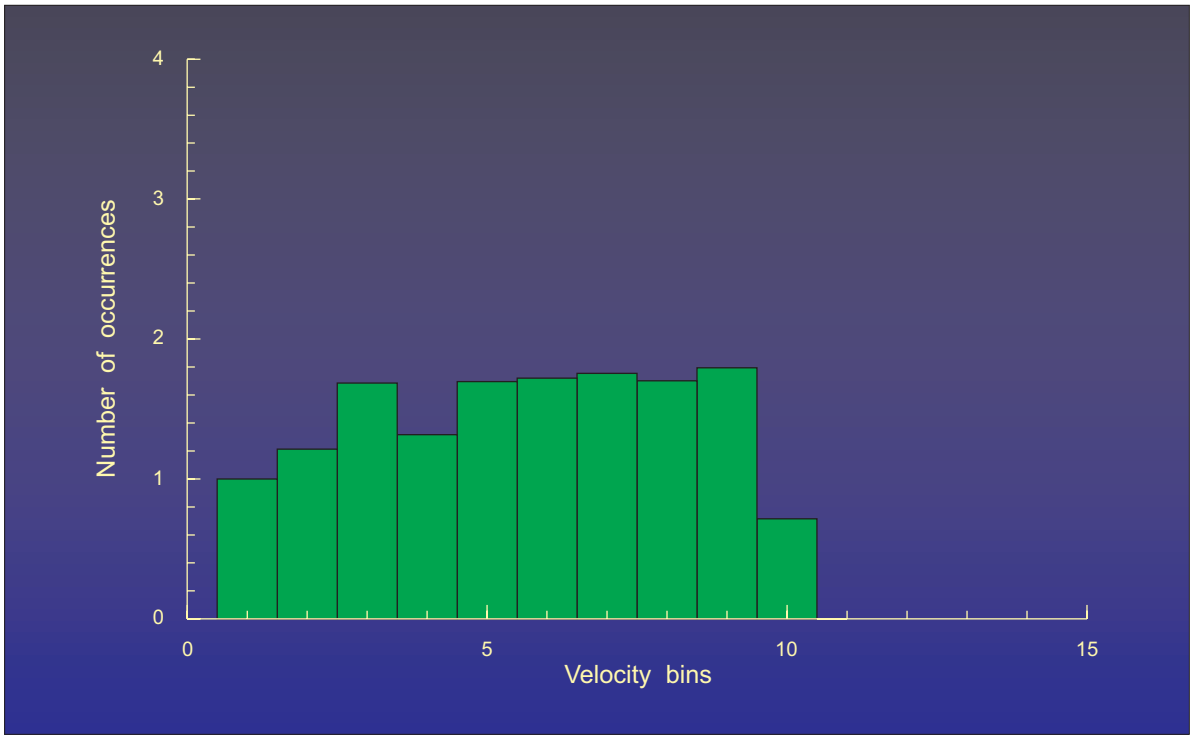

Figure 18.- Occurrence histogram of *additional measurements* following the first velocity measurement within a Taylor time microscale obtained at the edge of the pipe flow jet, 12 cm downstream from the pipe exit.

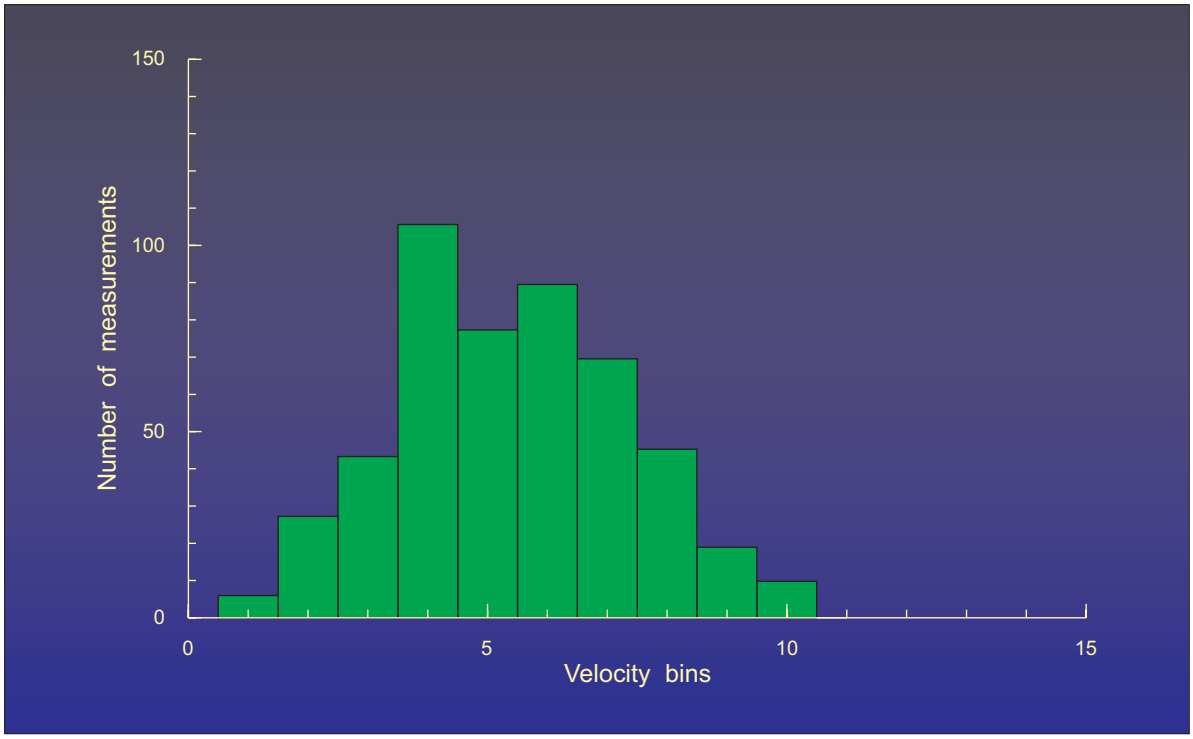

Figure 19.- Histogram of independent velocities obtained at the edge of the pipe flow jet, 12 cm downstream from the pipe exit.

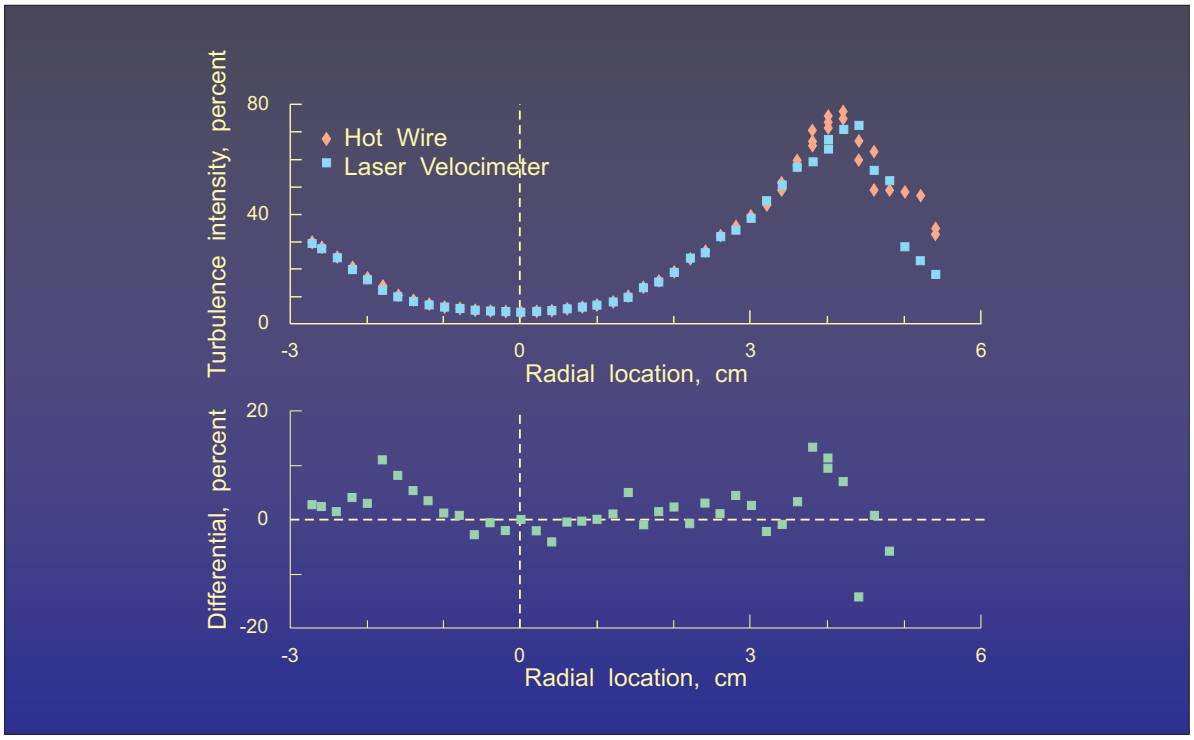

Figure 20.- Comparison of corrected (histogram processing - Edwards and Meyers) laser velocimeter and hot wire turbulence intensity measurements along a radial scan 12 cm downstream from the pipe exit.

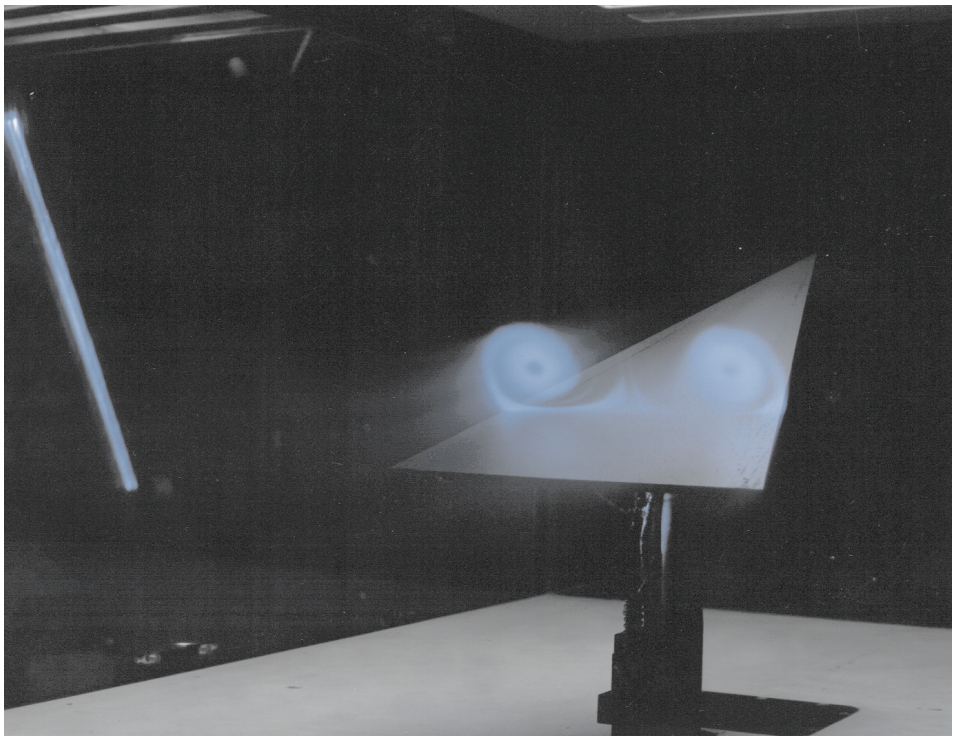

Figure 21.- Laser light sheet visualization of the leading edge vortex flow field above a 75^{o} delta wing at 20.5^{o} angle of attack at an $x/L = 0.7$.

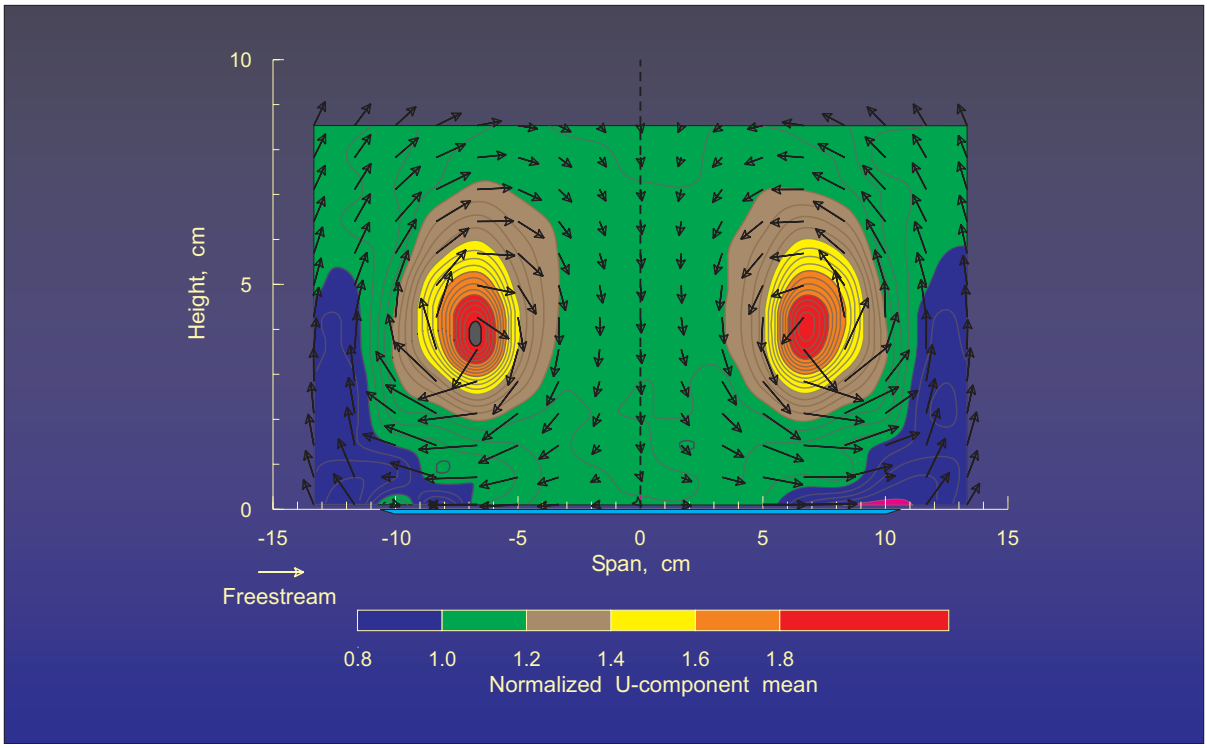

Figure 22.- Three component velocity measurements of the leading edge vortex flow field above a 75^{o} delta wing at 20.5^{o} angle of attack at an $x/L = 0.7$.

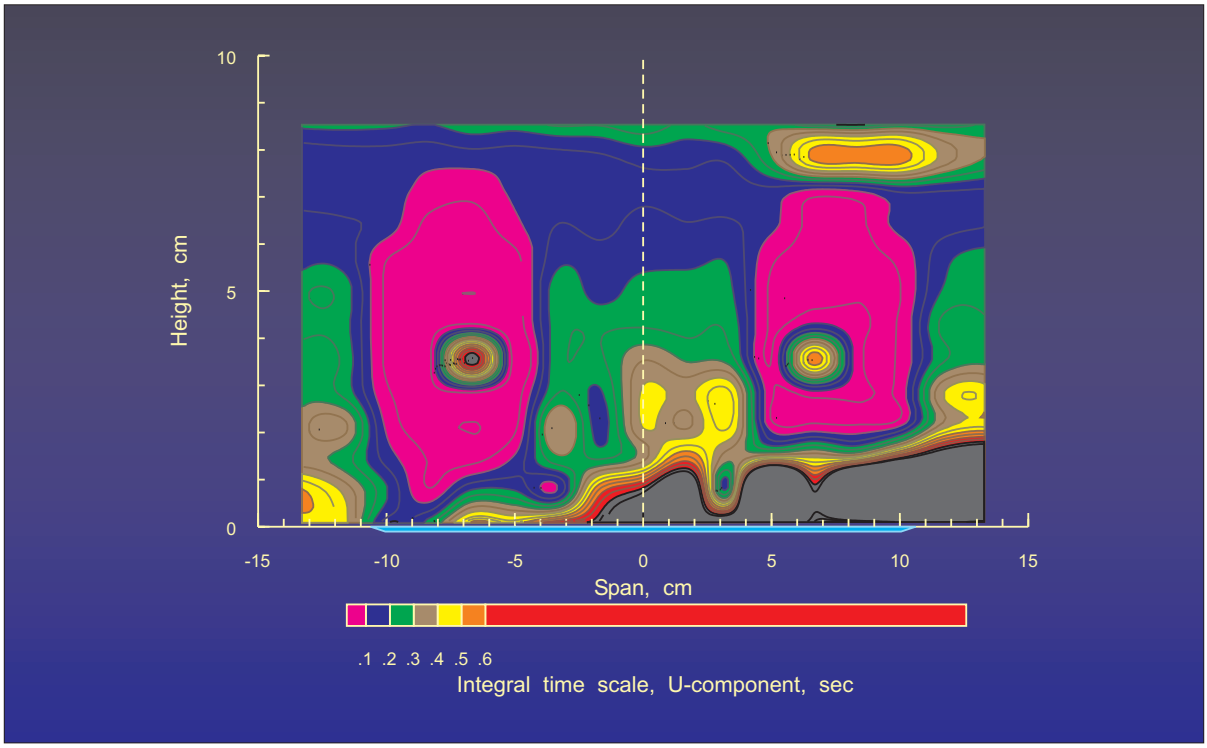

Figure 23.- Estimated Taylor time microscales of the leading edge vortex flow field above a 75^{o} delta wing at 20.5^{o} angle of attack at an $x/L = 0.7$.

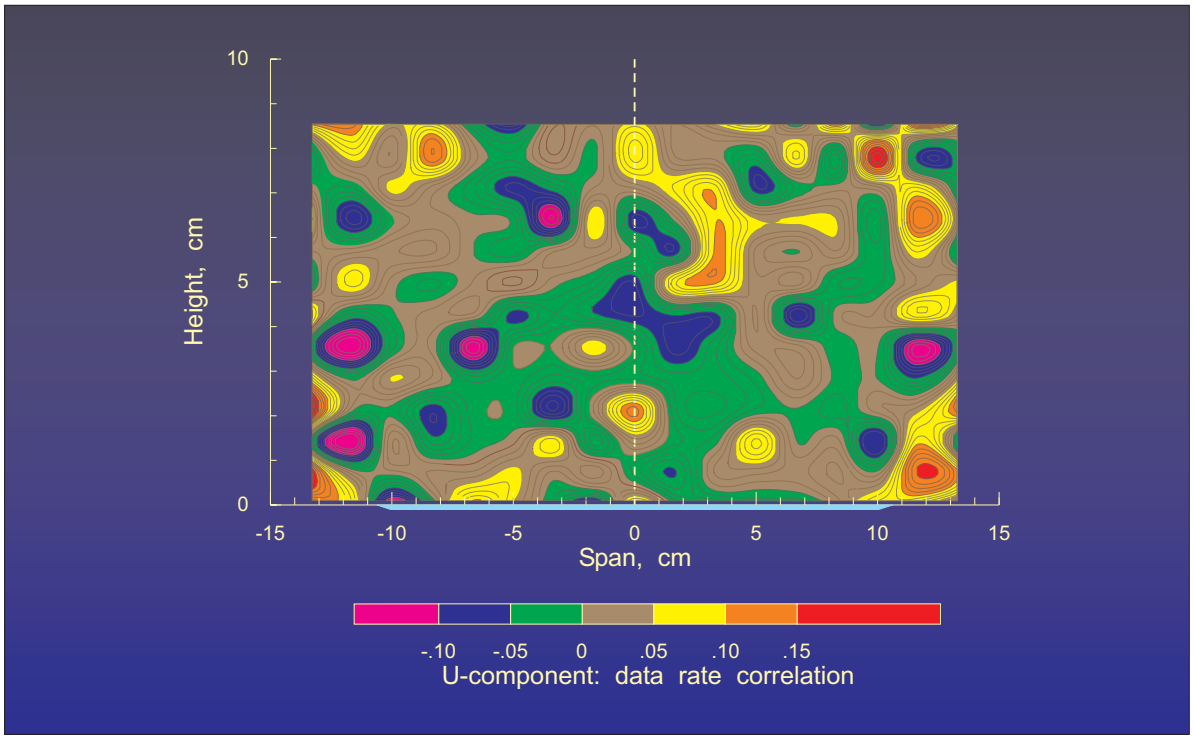

Figure 24.- *U*-component velocity : data rate correlation coefficients of the leading edge vortex flow field above a 75^{o} delta wing at 20.5^{o} angle of attack at an $x/L = 0.7$.

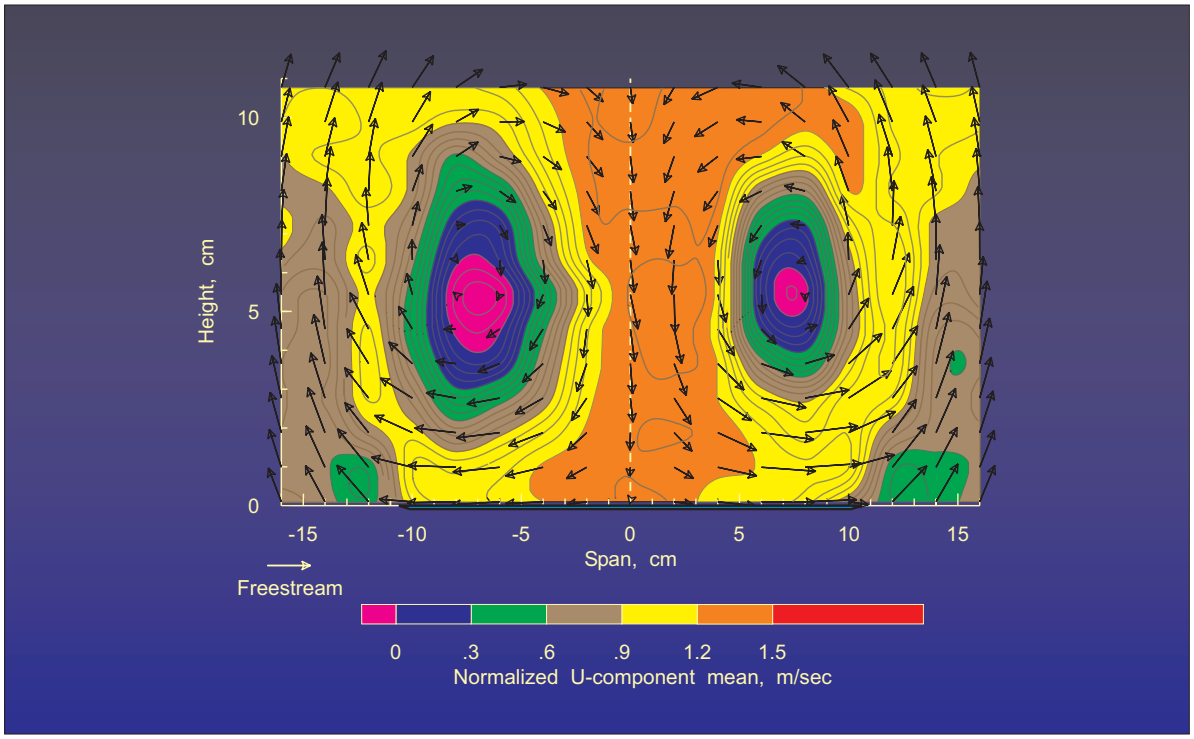

Figure 25.- Three component velocity measurements of the leading edge vortex flow field above a 75^{o} delta wing at 40.0^{o} angle of attack at an $x/L = 0.7$.

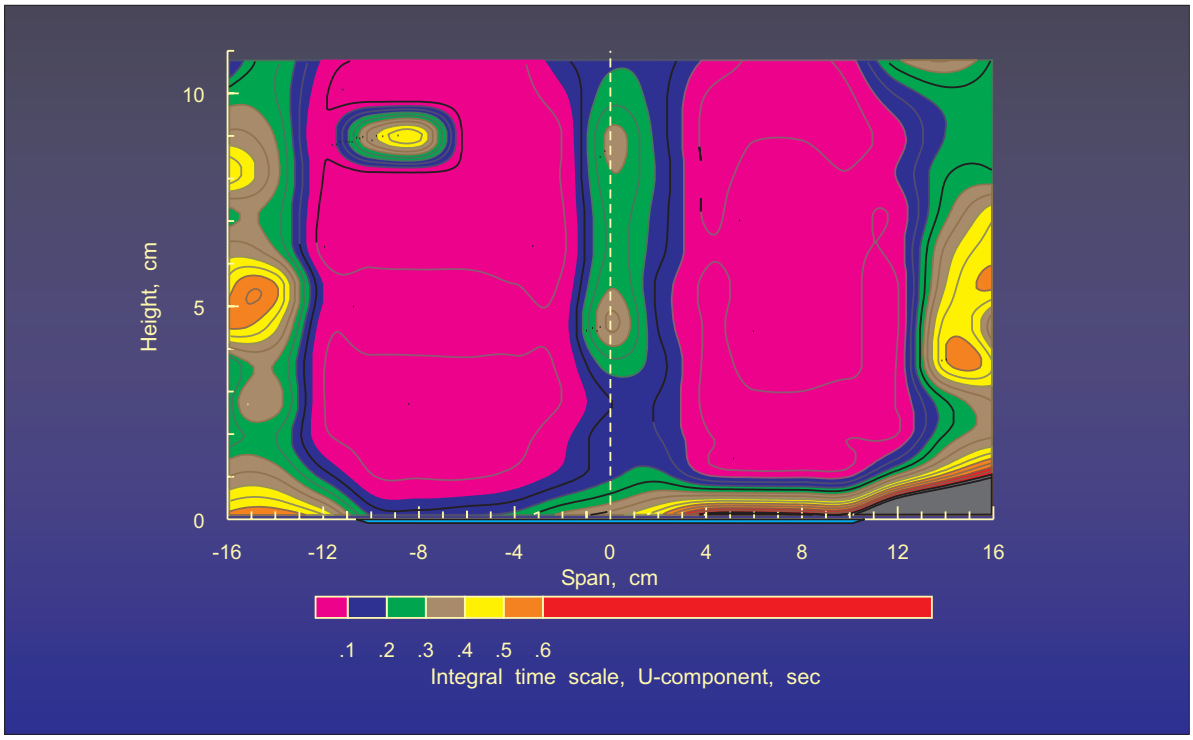

Figure 26.- Estimated Taylor time microscales of the leading edge vortex flow field above a 75^{o} delta wing at 40.0^{o} angle of attack at an $x/L = 0.7$.

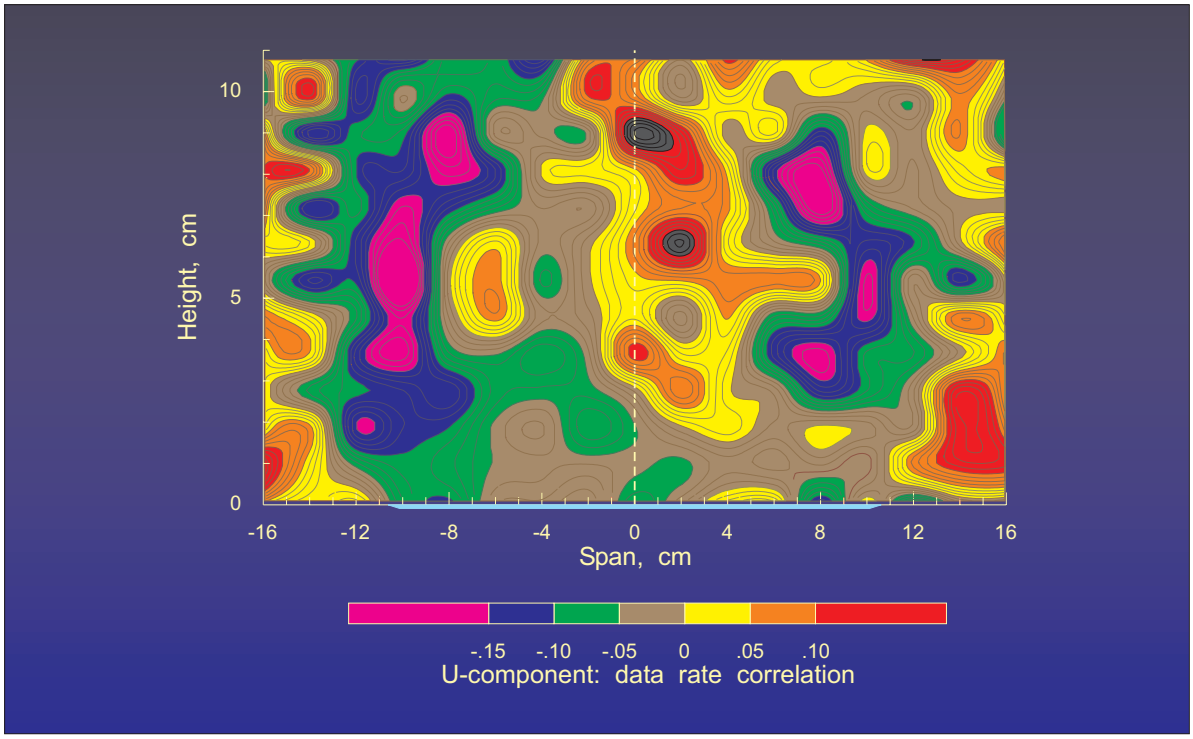

Figure 27.- *U*-component velocity : data rate correlation coefficients of the leading edge vortex flow field above a 75^{o} delta wing at 40.0^{o} angle of attack at an $x/L = 0.7$.

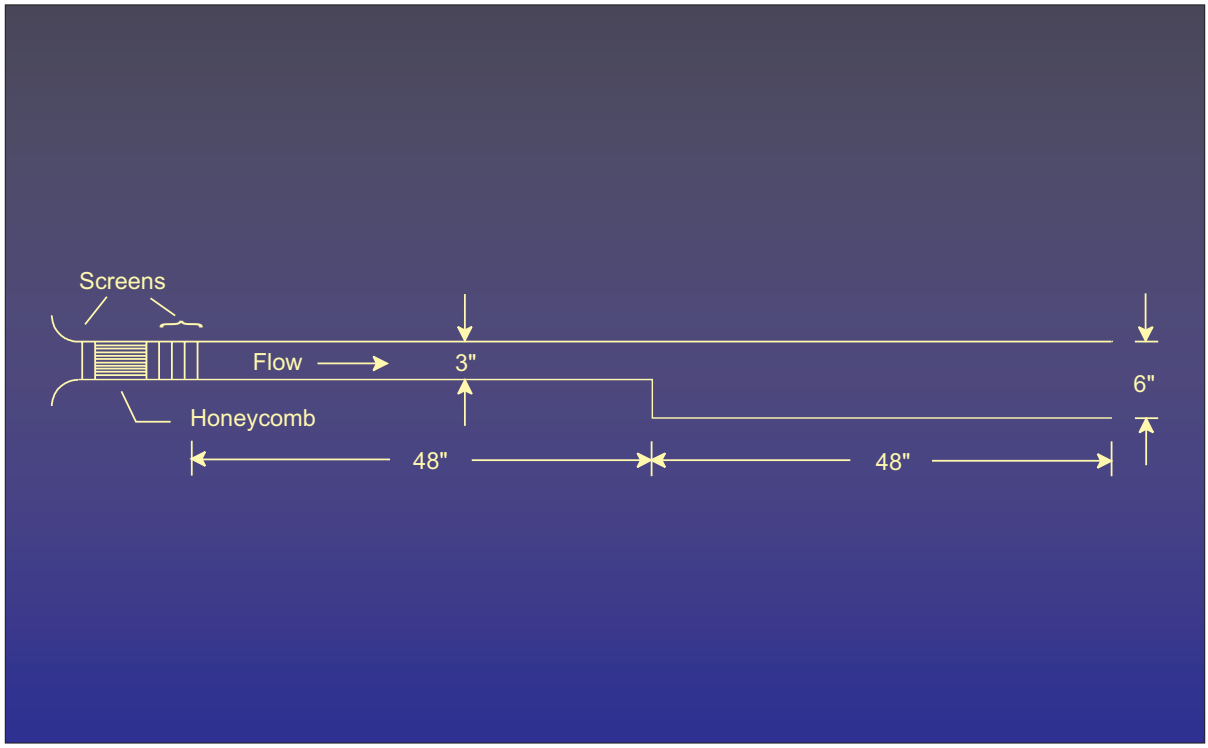

Figure 28.- Axial cross section of the backward facing step apparatus.

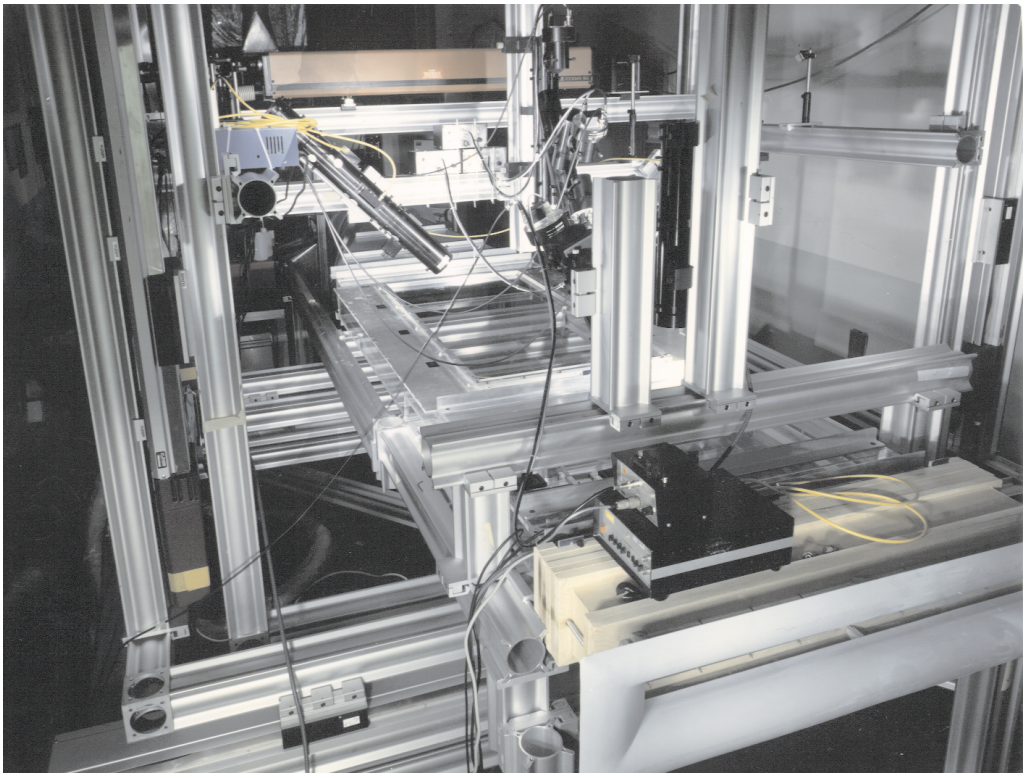

Figure 29.- The backward facing step apparatus and the four component laser velocimeter system installed on the traversing mechanism.

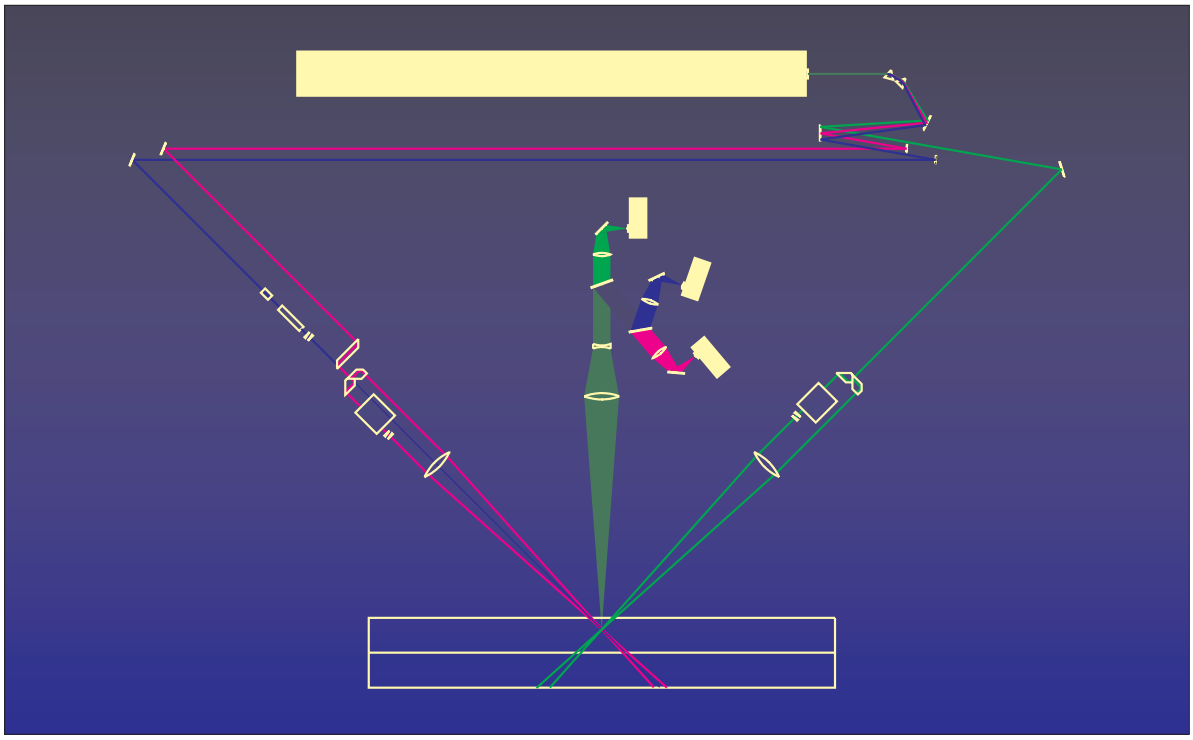

Figure 30.- Schematic of the three component laser velocimeter measurement system.

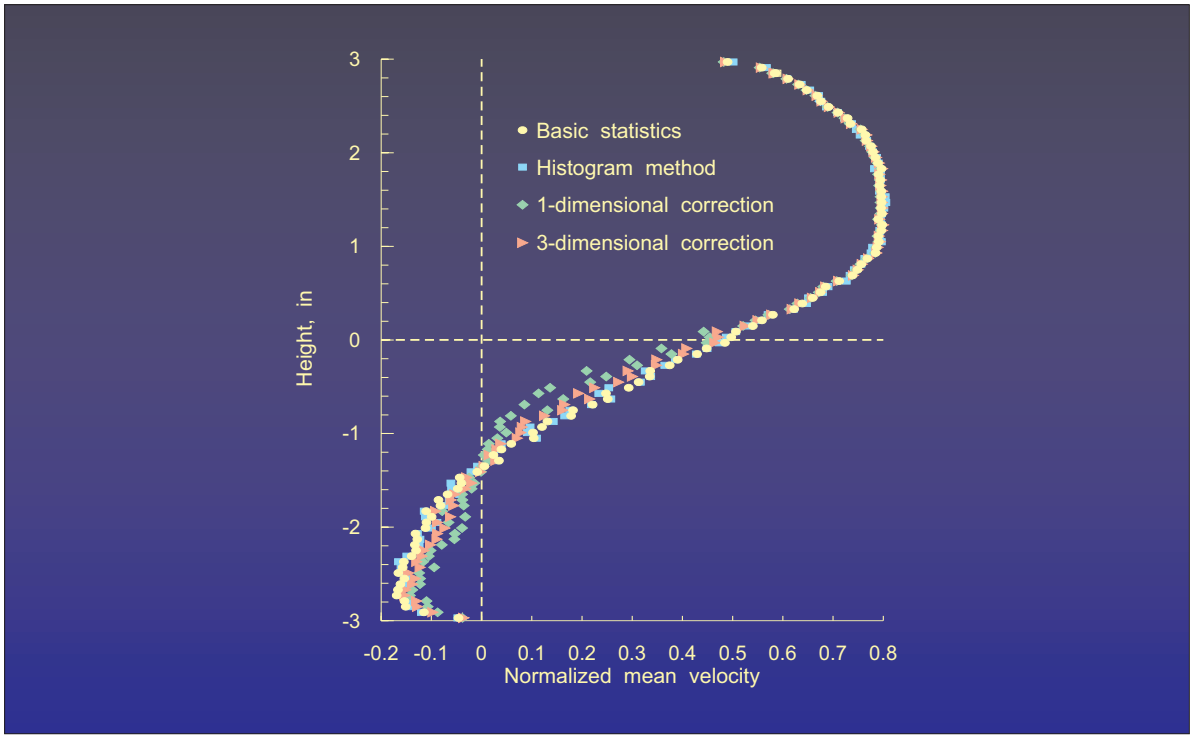

Figure 31.- Mean velocity measurements normalized by the free stream velocity upstream of the step along a vertical traverse, three step heights downstream of the backward facing step.

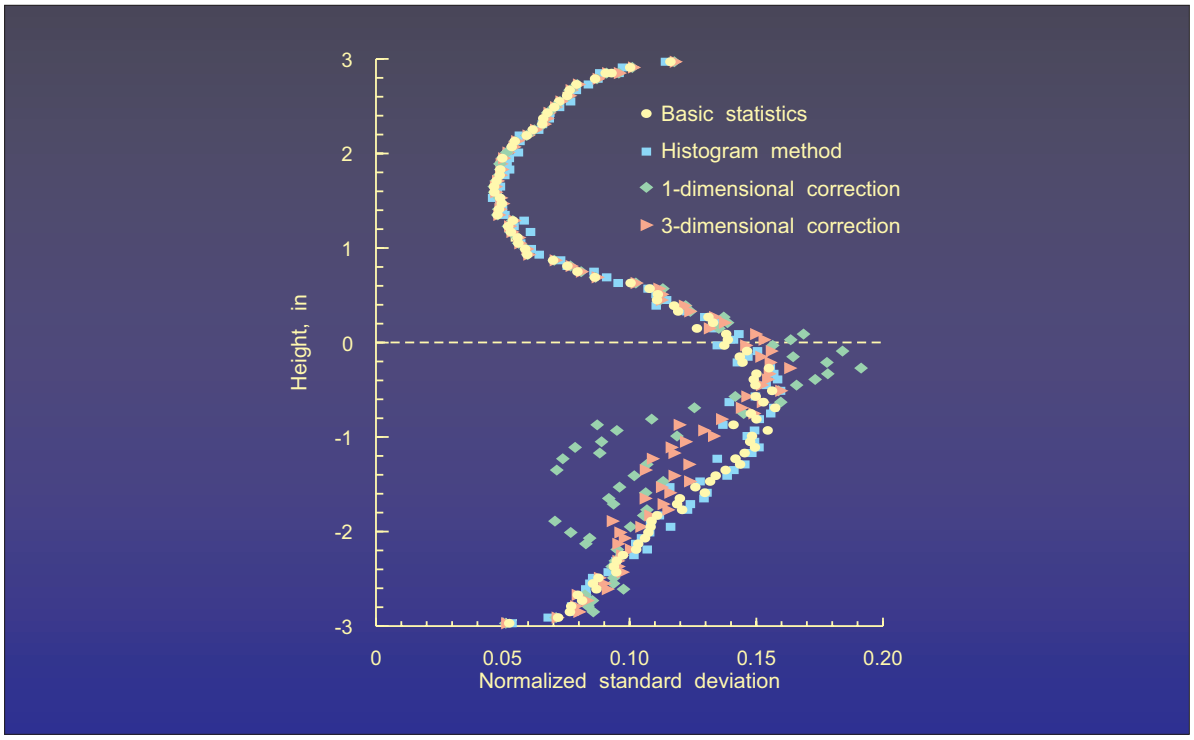

Figure 32.- Standard deviations of velocity normalized by the free stream velocity upstream of the step along a vertical traverse, three step heights downstream of the backward facing step.

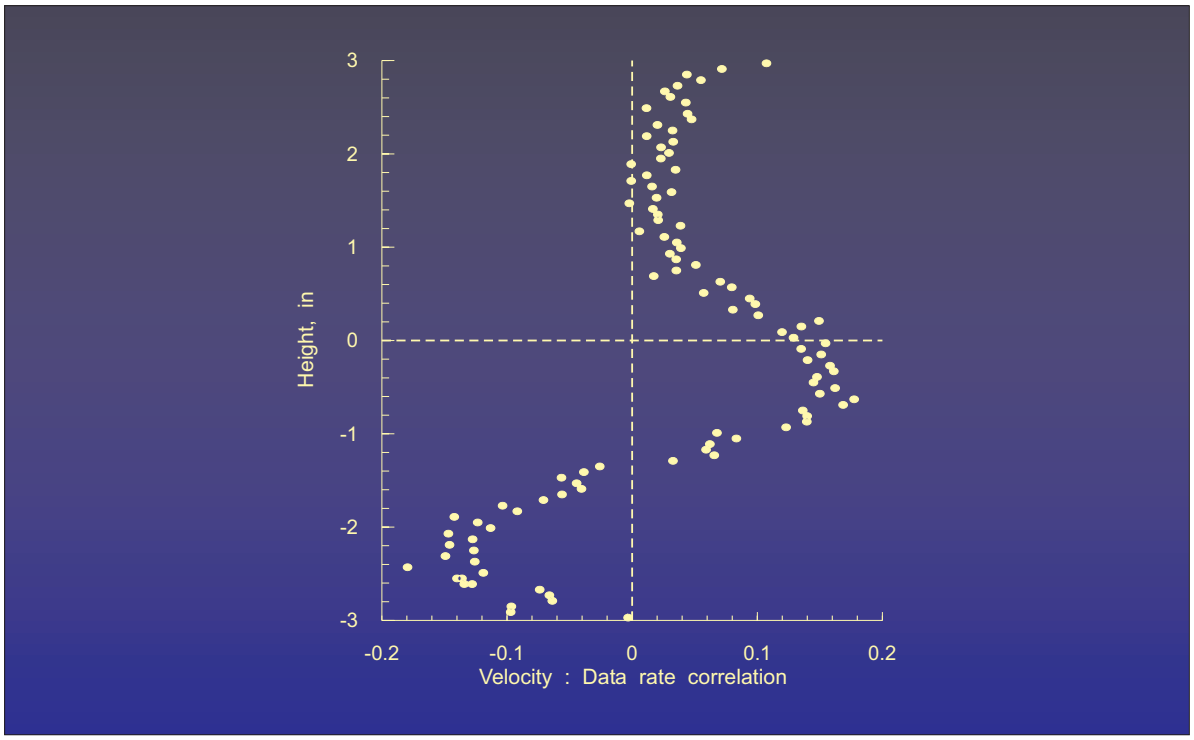

Figure 33.- Velocity : data rate correlation coefficients along a vertical traverse, three step heights downstream of the backward facing step.

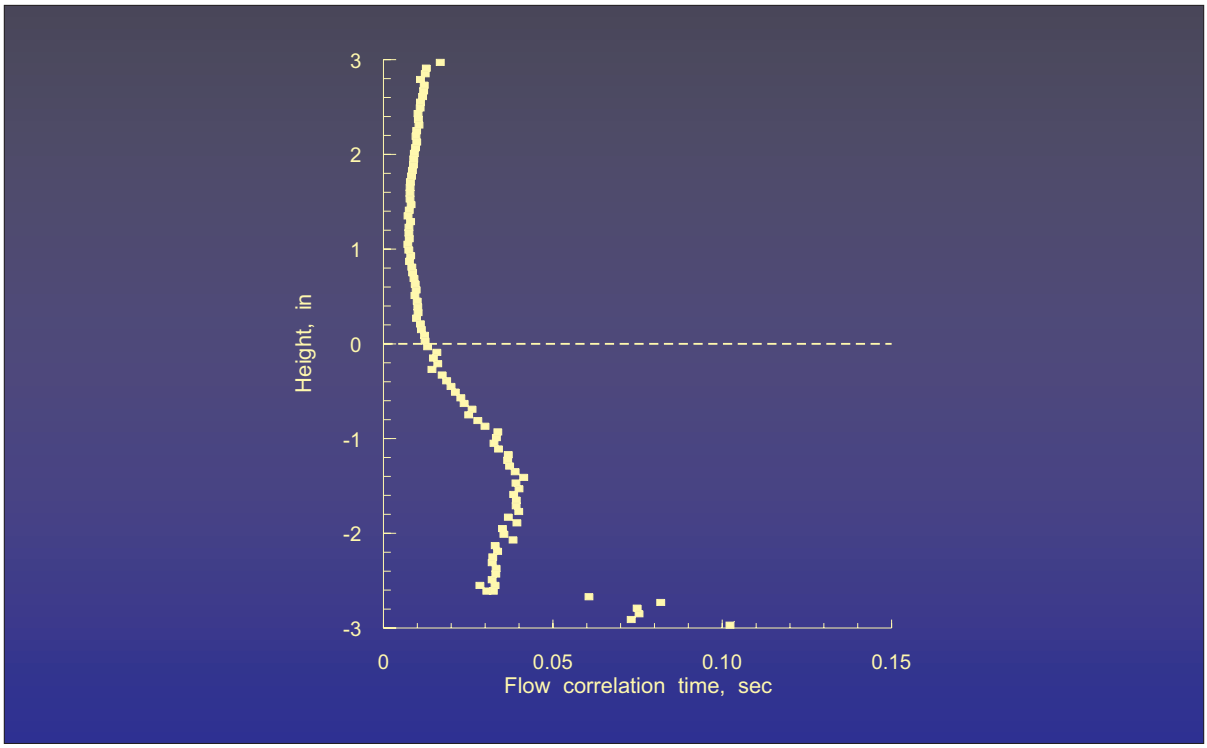

Figure 34.- Estimated Taylor time microscales along a vertical traverse, three step heights downstream of the backward facing step.

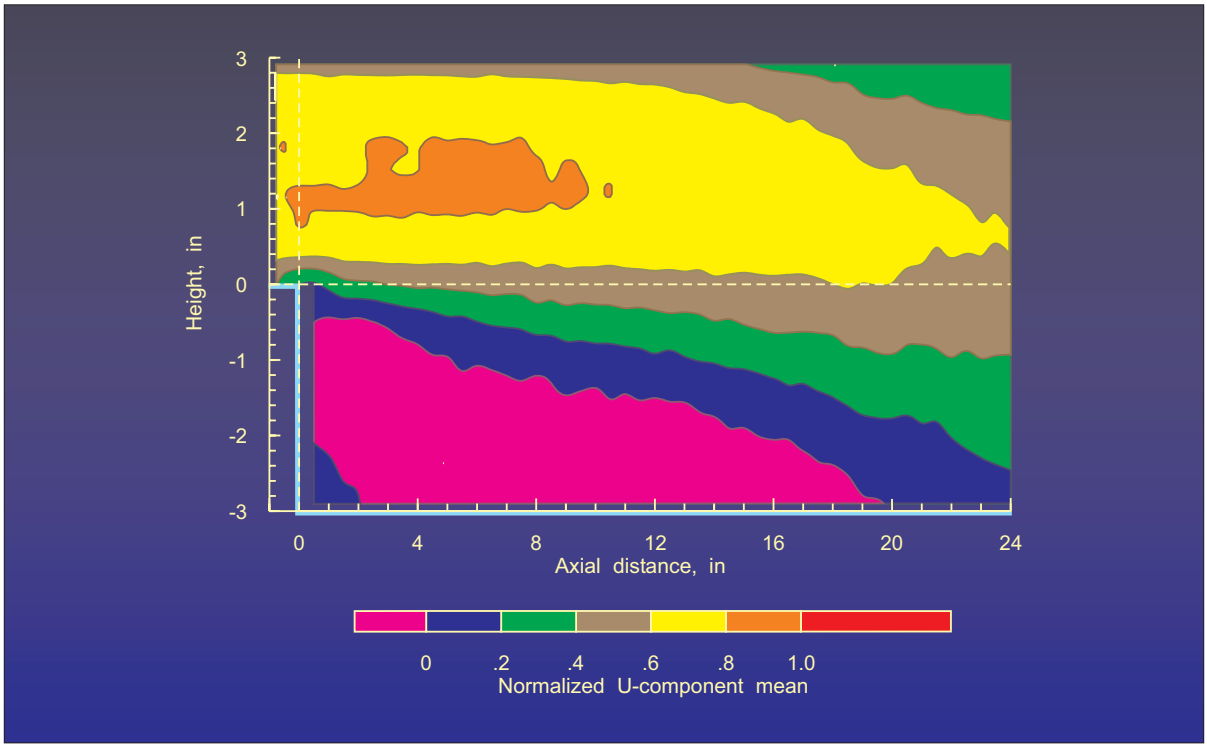

Figure 35.- Mean velocity flow field map about the backward facing step using basic statistical data processing.

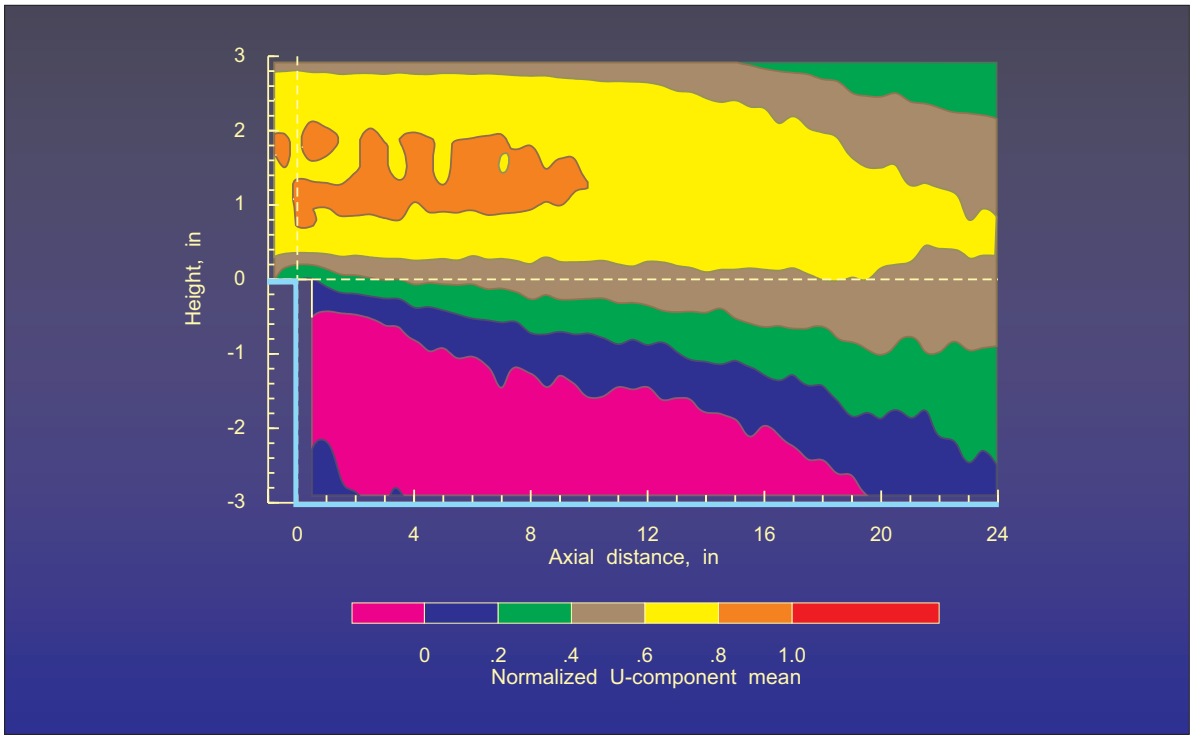

Figure 36.- Mean velocity flow field map about the backward facing step using the histogram method of data processing developed by Edwards and Meyers.

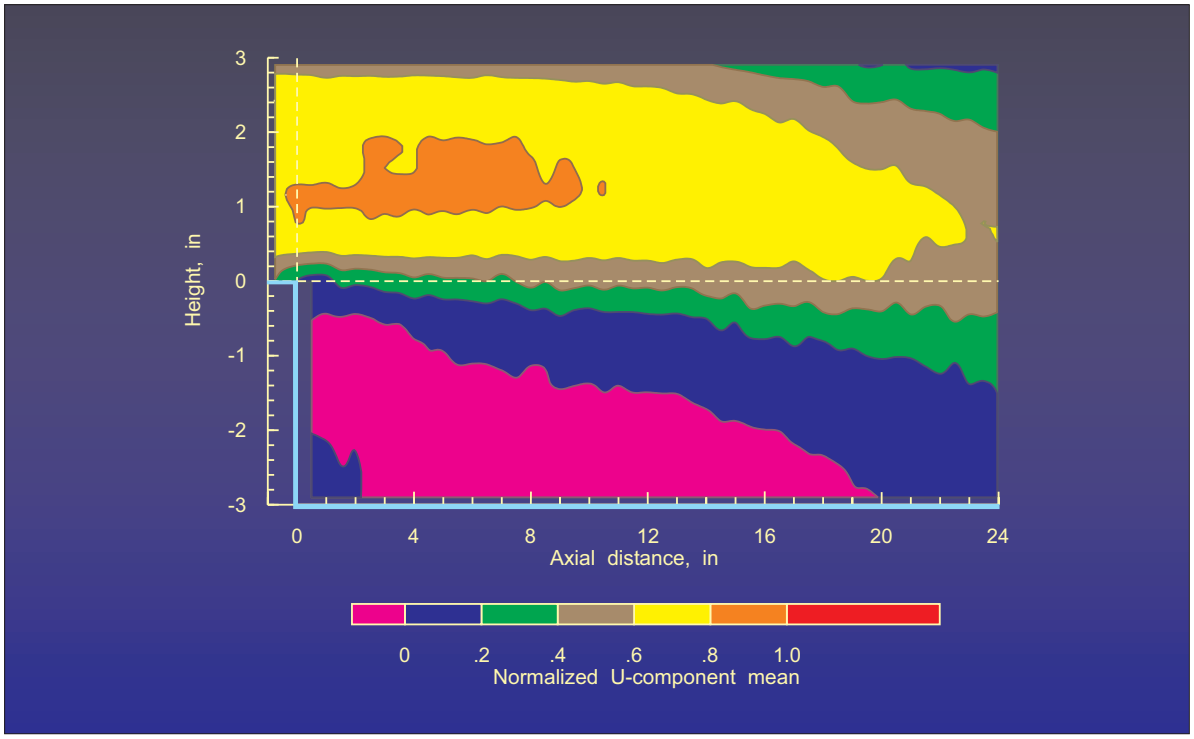

Figure 37.- Mean velocity flow field map about the backward facing step with the basic statistical data corrected using the classic 1-dimensional velocity bias correction technique developed by McLaughlin and Tiedermann.

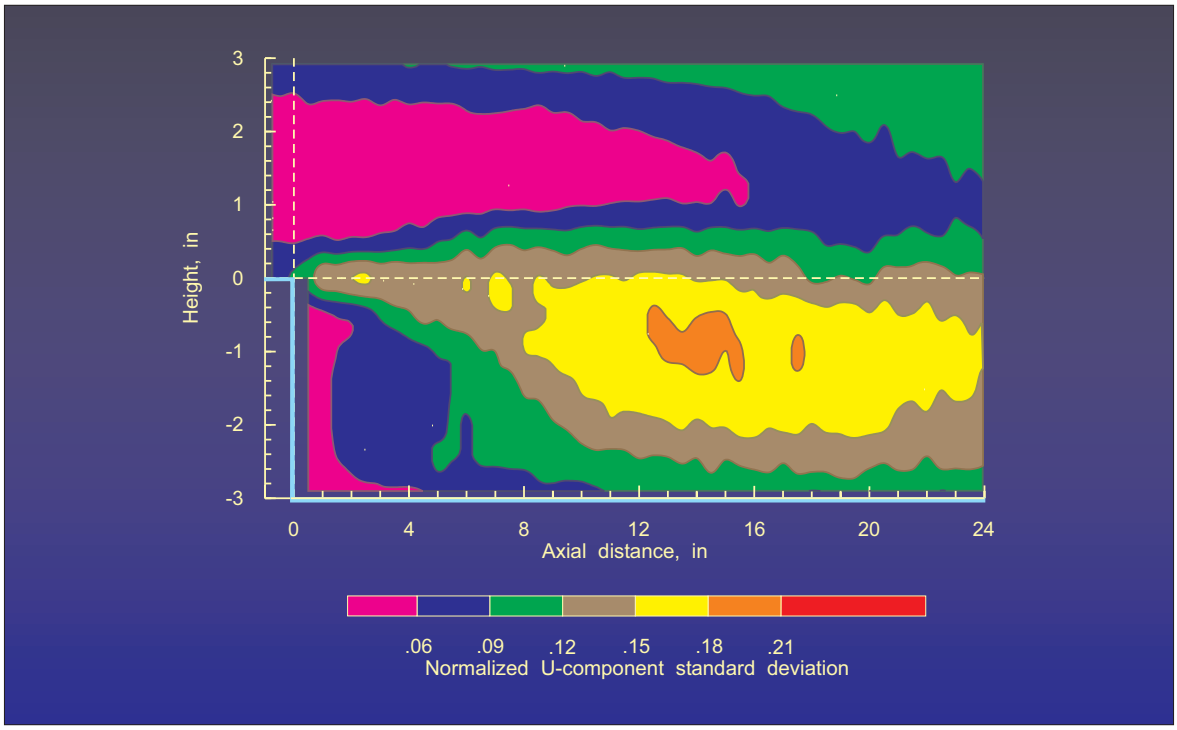

Figure 38.- Flow field map of standard deviation of velocity normalized by the local mean velocity about the backward facing step using basic statistical data processing.

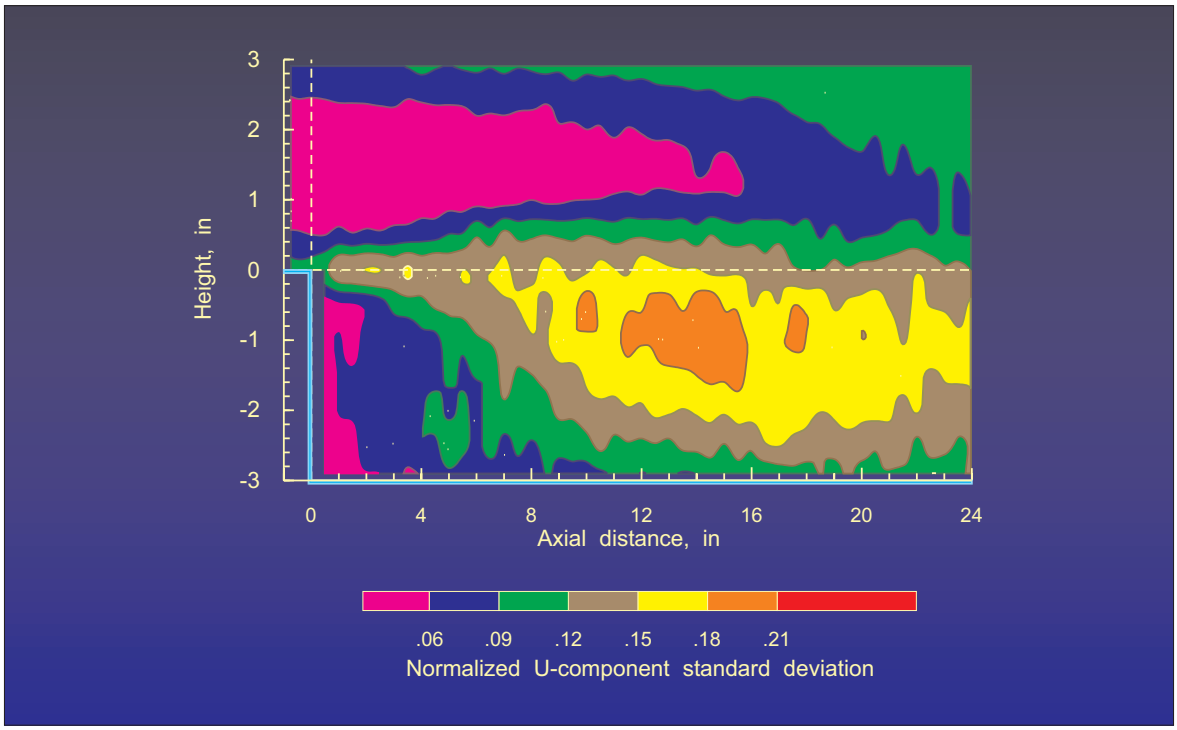

Figure 39.- Flow field map of standard deviation of velocity normalized by the local mean velocity about the backward facing step using the histogram method of data processing developed by Edwards and Meyers.

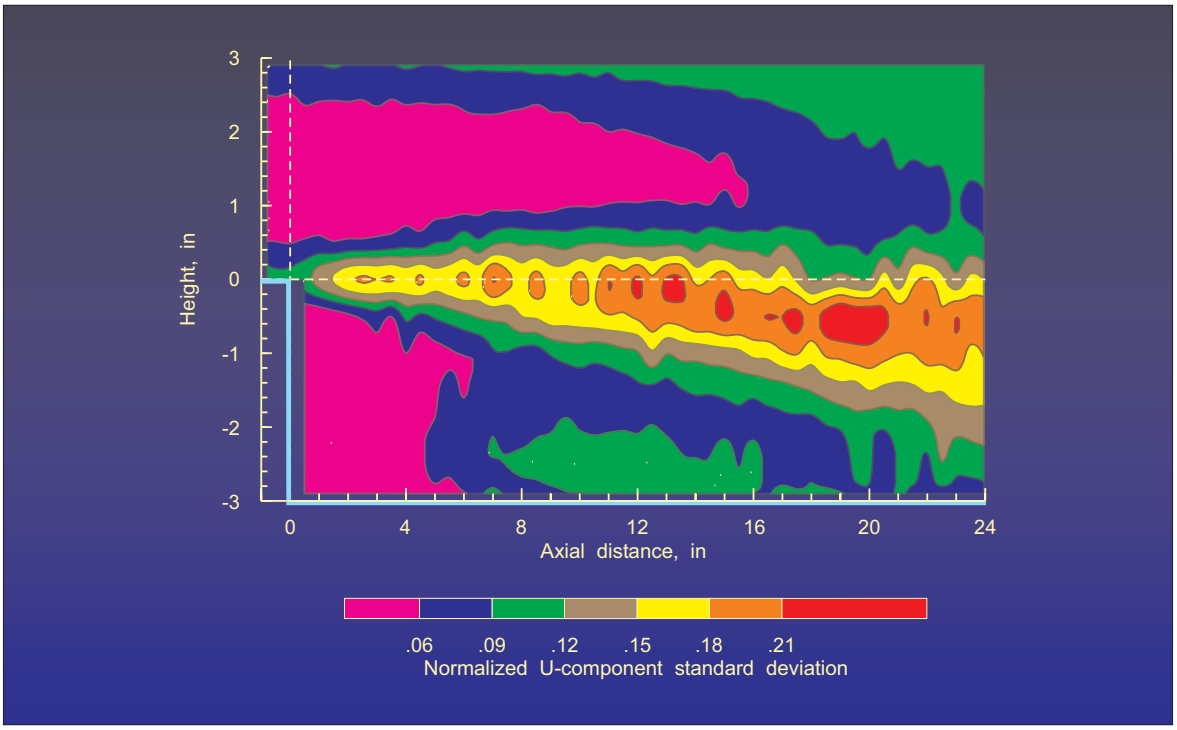

Figure 40.- Flow field map of standard deviation of velocity normalized by the local mean velocity about the backward facing step with the basic statistical data corrected using the classic 1-dimensional velocity bias correction technique developed by McLaughlin and Tiedermann.

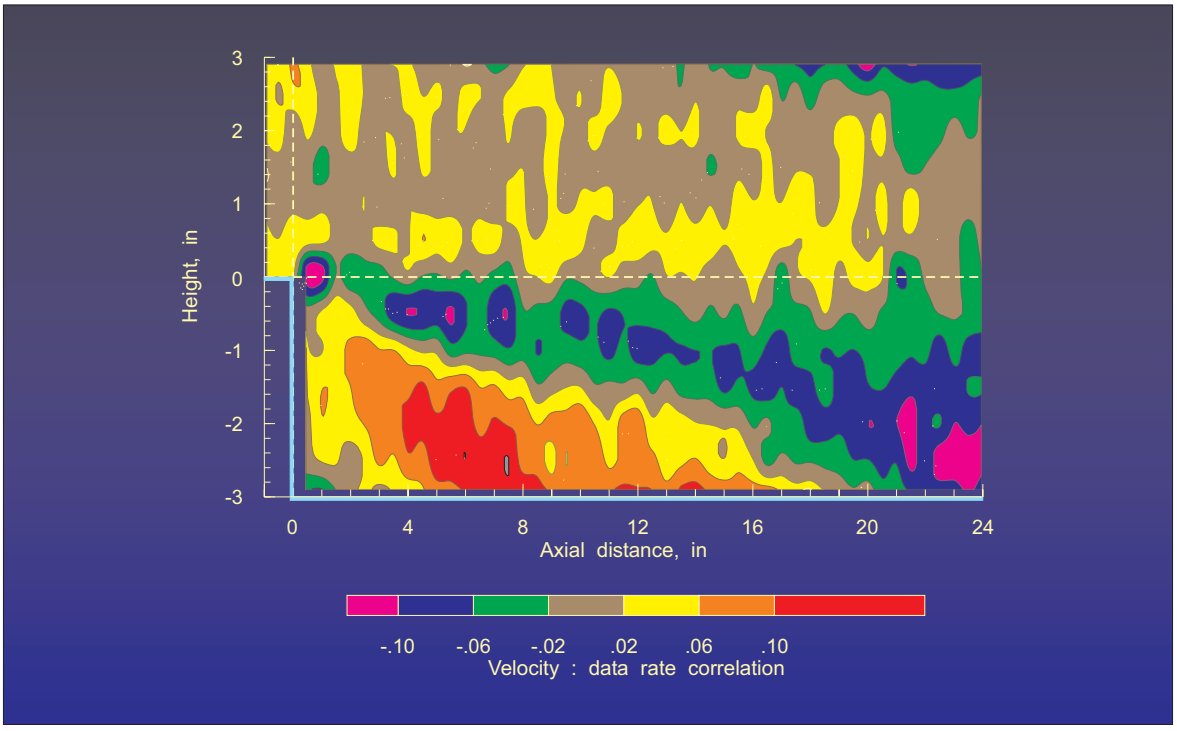

Figure 41.- Map of the velocity : data rate correlation coefficients about the backward facing step.

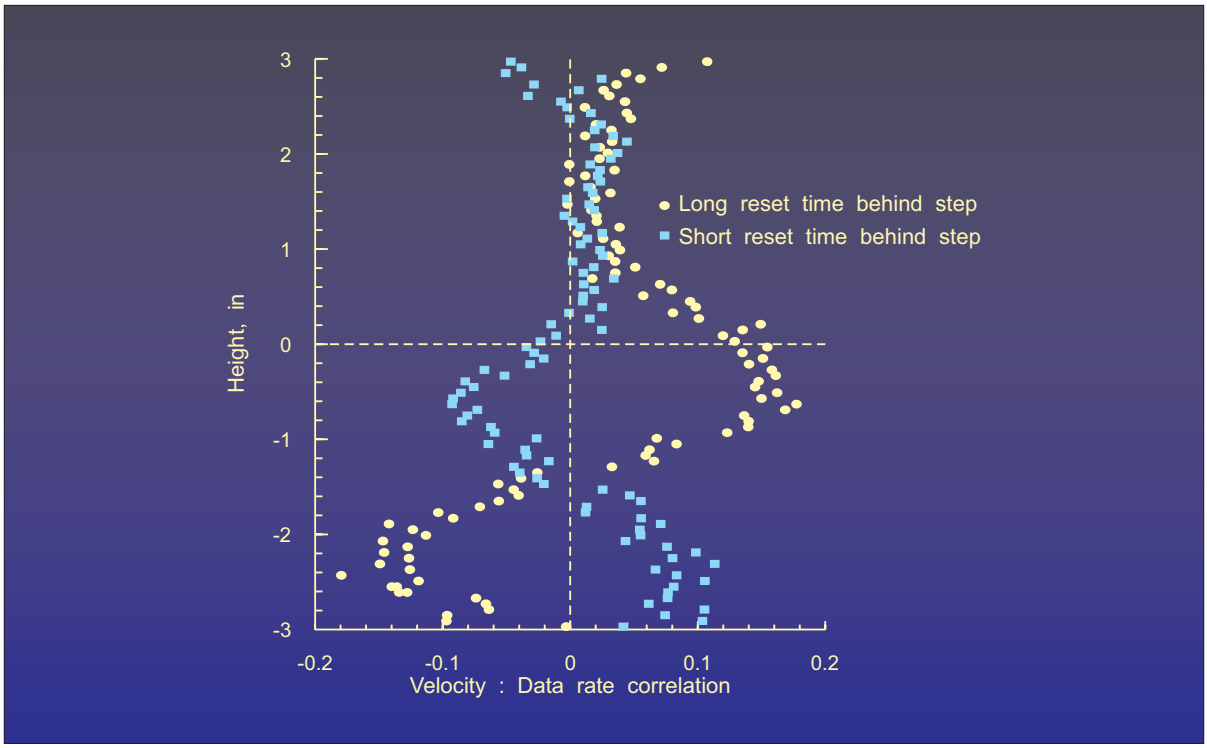

Figure 42.- Comparison of velocity : data rate correlation coefficients along a vertical traverse three step heights downstream of the backward facing step.